BACTERIOLOGY

10.1126/sciadv.1400225

Mast cell degranulation by a hemolytic lipid toxin decreases GBS colonization and infection

Claire Gendrin,[1,2] Jay Vornhagen,[2,3] Lisa Ngo,[2] Christopher Whidbey,[2,3] Erica Boldenow,[2] Veronica Santana-Ufret,[2] Morgan Clauson,[2] Kellie Burnside,[1]* Dionne P. Galloway,[4†] Kristina Adams Waldorf,[4] Adrian M. Piliponsky,[1,2‡] Lakshmi Rajagopal[1,2,3‡]

Ascending infection of microbes from the lower genital tract into the amniotic cavity increases the risk of preterm birth, stillbirth, and newborn infections. Host defenses that are critical for preventing ascending microbial infection are not completely understood. Group B *Streptococcus* (GBS) are Gram-positive bacteria that frequently colonize the lower genital tract of healthy women but cause severe infections during pregnancy, leading to preterm birth, stillbirth, or early-onset newborn infections. We recently described that the GBS pigment is hemolytic, and increased pigment expression promotes GBS penetration of human placenta. Here, we show that the GBS hemolytic pigment/lipid toxin and hyperpigmented GBS strains induce mast cell degranulation, leading to the release of preformed and proinflammatory mediators. Mast cell–deficient mice exhibit enhanced bacterial burden, decreased neutrophil mobilization, and decreased immune responses during systemic GBS infection. In a vaginal colonization model, hyperpigmented GBS strains showed increased persistence in mast cell–deficient mice compared to mast cell–proficient mice. Consistent with these observations, fewer rectovaginal GBS isolates from women in their third trimester of pregnancy were hyperpigmented/hyperhemolytic. Our work represents the first example of a bacterial hemolytic lipid that induces mast cell degranulation and emphasizes the role of mast cells in limiting genital colonization by hyperpigmented GBS.

INTRODUCTION

Bacterial infection and inflammation are major causes of neonatal morbidity and mortality (*1*, *2*). Although pathogens such as Group B *Streptococcus* (GBS) reside as commensal organisms in the lower genital tract of women, ascending in utero infection or vertical transmission of GBS from the mother to the infant during labor and delivery results in invasive neonatal disease (*3*–*5*). The nature of immune cells that detect and either prevent or exacerbate ascending microbial infection is not understood. This lack of information imposes significant constraints on the development of preventive strategies that decrease the risk of preterm birth, stillbirth, and early-onset neonatal infections.

Mast cells are derived from hematopoietic progenitor cells and are widely distributed in tissues at the interface with the external environment including the lower genital tract (*6*). Unlike neutrophils or macrophages that are recruited to the site of infection, mast cells are resident immune sentinel cells that exist in high numbers in the vagina and cervix (*6*, *7*) and can come into contact with pathogens early during colonization/infection (*8*–*10*). Mast cells degranulate when stimulated, resulting in the rapid release of preformed mediators present in cytoplasmic granules such as histamine, preformed tumor necrosis factor (TNF), and proteases including tryptase and chymase; histamine release has been linked to neutrophil recruitment and the generation of a proinflammatory response (*11*–*13*). Activated mast cells also produce lipid-derived eicosanoids such as prostaglandin D_2 (PGD_2) and leukotriene C_4 (LTC_4), and over the course of hours, mast cells release chemokines and cytokines including interleukin-6 (IL-6) (*8*–*10*). Although primarily recognized for their role in immunoglobulin E (IgE)–associated allergic disorders, mast cells can contribute to the generation of a proinflammatory microenvironment in response to invading pathogens. This proinflammatory response can either curtail the infection or conversely exacerbate the inflammatory response, leading to mortality as observed in severe infections (*9*, *14*). Recently, however, mast cell release of IL-4 has been indicated to dampen macrophage phagocytosis and aggravate sepsis in a murine model of cecal ligation and puncture (*15*). The role of mast cells in the regulation of GBS colonization and infection is not known.

We recently described that the hemolytic pigment of GBS promotes bacterial penetration of human placenta and that hyperpigmented strains can be isolated from women in preterm labor (*16*). Here, we show that the hemolytic GBS pigment triggers mast cell degranulation, resulting in the release of preformed and proinflammatory mediators. We also show that mast cell degranulation due to hyperpigmented/hypervirulent GBS decreases systemic virulence and diminishes vaginal colonization. These results suggest that mast cell degranulation in the lower genital tract can limit colonization of hyperpigmented GBS strains.

RESULTS

Fewer hyperhemolytic GBS were isolated from the lower genital tract of pregnant women

We recently showed that the molecular basis for GBS hemolytic activity is the ornithine rhamnolipid pigment or lipid toxin (*16*). We also described that hyperpigmented GBS, some of which were associated with mutations in a two-component repressor of the hemolytic pigment known as CovR/CovS (comprising the sensor kinase CovS and the DNA binding response regulator CovR), were present in the amniotic

[1]Department of Pediatric Infectious Diseases, University of Washington, Seattle, WA 98101, USA. [2]Seattle Children's Research Institute, Seattle, WA 98101, USA. [3]Department of Global Health, University of Washington, Seattle, WA 98195, USA. [4]Department of Obstetrics and Gynecology, University of Washington, Seattle, WA 98195, USA.
*Present address: LabCorp Clinical Trials, Seattle, WA 98109, USA.
†Present address: Women's Health Centre, Morehead Memorial Hospital, Eden, NC 27288, USA.
‡Corresponding author. E-mail: lakshmi.rajagopal@seattlechildrens.org (L.R.); adrian.piliponsky@seattlechildrens.org (A.M.P.)

fluid and placental membranes of women in preterm labor (*16*), and can induce fetal injury (*17*). To determine if hyperhemolytic GBS exist as colonizers in the lower genital tract of adult women, we analyzed GBS isolates obtained from rectovaginal swabs of 53 women in their third trimester of pregnancy. GBS strains were examined for their hemolytic properties and pigmentation on blood agar and tryptic soy agar (TSA), respectively. As controls, the wild-type GBS strain COH1 and isogenic Δ*covR*, which exhibits increased hemolysis/pigmentation, were used; these controls were chosen because they were used in our previous work (*16*) to compare hyperhemolysis/pigmentation from GBS obtained from women in preterm labor. Quantitative titers were estimated using a modified hemolysis assay (see Materials and Methods). We observed that 2 of the 53 isolates showed increased hemolysis/pigmentation similar to Δ*covR* (Table 1 and fig. S1). In comparison, we previously obtained eight GBS isolates obtained from six women in preterm labor and subsequently noted that these were hyperhemolytic (*16*). Although our collection of GBS clinical isolates is not exhaustive, the frequency of hyperhemolysis that we observed between the GBS preterm (8 of 8) and rectovaginal isolates (2 of 53) is significantly different ($P = 0.001$, Fisher's exact test). These observations suggest that host immune mechanisms may diminish colonization of hypervirulent/hyperpigmented GBS strains from the vaginal microenvironment. Whereas the two hyperhemolytic rectovaginal isolates resembled the Δ*covR* strain in other phenotypic properties [for example, decreased expression of CovR-activated CAMP factor; Table 1 and fig. S1 (*18*–*20*)], DNA sequencing of the *covR/S* locus did not reveal the presence of any mutations, similar to the previously described natively hyperpigmented strain NCTC10/84 (*21*–*23*). These results suggest that the presence of other regulators may influence the expression of the *covR/S* regulon in certain GBS strains. Nevertheless, these observations led us to hypothesize that an effective host immune response may diminish colonization of hypervirulent/hyperpigmented GBS strains from the human vaginal microenvironment.

Table 1. Hemolytic titers of GBS strains isolated from rectovaginal swabs of women in their third trimester of pregnancy. COH1 is a wild-type GBS clinical isolate from an infected newborn and belongs to the hypervirulent ST-17 clone. COH1Δ*covR* is a mutant derived from COH1 and exhibits increased hemolytic activity. Strains #65 and #91 are rectovaginal GBS isolates that exhibit increased hemolysis and decreased CAMP factor expression similar to COH1Δ*covR* (see fig. S1).

Strain	Hemolytic titer
Clinical isolates	
Wild-type GBS (COH1)	2
Δ*covR*	>32
Rectovaginal isolates	
Strain #65	>32
Strain #91	>32
Remaining 51 isolates	≤2

The hemolytic pigment of GBS triggers the release of preformed and proinflammatory mediators from mast cells

To gain further understanding of how the human host may preferentially eradicate hyperpathogenic/hyperpigmented GBS from the lower genital tract, we examined the role of mast cells. Because mast cells are resident immune cells in the lower genital tract, we hypothesized that mast cell activation may contribute to decreased vaginal colonization of hyperhemolytic/hyperpigmented GBS. To test this hypothesis, we first examined if the GBS hemolytic pigment induced mast cell degranulation. For these studies, we used both bone marrow and peritoneal mast cells as model systems because they represent mucosal and connective tissue mast cells that are found in vivo and, in some instances, can have differential activation (*24*). Bone marrow–derived mast cells (BMCMCs) and peritoneal cell–derived mast cells (PCMCs) were isolated from wild-type mice (C57BL6/J) and cultured in vitro as described (*25*, *26*) until mast cells represented >90% of the total nonadherent cells. Flow cytometric analysis of the in vitro cultured PCMCs confirmed the presence of the mast cell surface receptors FcεRI and c-kit (CD117; fig. S2). Similar results were obtained with BMCMCs (data not shown). The generated mast cells were then exposed to varying concentrations of purified GBS hemolytic pigment (0.625 to 7.5 μM) for 1 hour. Controls included an equivalent amount of extract from nonpigmented GBS (that is, Δ*cylE* extract), DTS buffer [dimethyl sulfoxide (DMSO) + 0.1% trifluoroacetic acid (TFA) + 20% starch], or 5 μM of the Ca^{2+} ionophore A23187 (see Materials and Methods for details). To assess mast cell degranulation, we determined the release of β-hexosaminidase (β-hex), a mast cell granule–derived enzyme, as described (*25*, *26*). We observed that the GBS pigment induced a significant release of β-hex from both BMCMCs (Fig. 1A) and PCMCs (Fig. 1B), similar to the Ca^{2+} ionophore A23187–stimulated positive controls. Release of β-hex was not observed in mast cells (BMCMCs) treated with the nonhemolytic pigment [that is, pigment lacking the carrier molecule starch (*17*); see fig. S3A] or when the β-hex substrate was omitted in mast cells treated with hemolytic pigment (data not shown). Together, these data confirm that the GBS hemolytic pigment triggers the release of β-hex from mast cells.

We next examined if GBS strains induce mast cell degranulation, similar to the purified pigment. In these studies, we included wild-type GBS (strain A909), isogenic hyperpigmented/hyperhemolytic Δ*covR*, and nonhemolytic/nonpigmented Δ*covR*Δ*cylE* and Δ*cylE* strains that lack the *cylE* gene necessary for hemolytic pigment biosynthesis (*16*, *21*). BMCMCs and PCMCs were treated for 1 hour with 10^7 colony-forming units (CFU) of GBS (wild-type A909, Δ*covR*, Δ*covR*Δ*cylE*, or Δ*cylE*), and the release of β-hex was measured. The results shown in Fig. 1, C and D, indicate that similar to the hemolytic pigment, hyperpigmented GBS (that is, Δ*covR*) induced the release of β-hex from both BMCMCs and PCMCs. Furthermore, the natively occurring hyperpigmented wild-type GBS strain NCTC10/84 induced the release of β-hex from mast cells, unlike the isogenic nonpigmented control NCTC10/84Δ*cylE* (fig. S3B). As hyperhemolytic GBS strains with mutations in *covS* were isolated from women in preterm labor (*16*), we also confirmed that GBS lacking CovS (Δ*covS*) induced the release of β-hex from mast cells unlike the isogenic nonpigmented control A909Δ*covS*Δ*cylX-K*, hereinafter called Δ*covS*Δ*cyl* (see fig. S3, C and D). Although hemolytic GBS strains have been described to activate the NLRP3 inflammasome in macrophages and dendritic cells (*27*, *28*), as does the purified pigment (*17*), we observed that the GBS pigment and hyperhemolytic Δ*covR* triggered the release of preformed mediators such as β-hex even from mast cells isolated from NLRP3 knockout mice (NLRP3KO; fig. S4), indicating that mast cell degranulation by the GBS pigment is independent of NLRP3 inflammasome activation. Collectively, these data confirm that

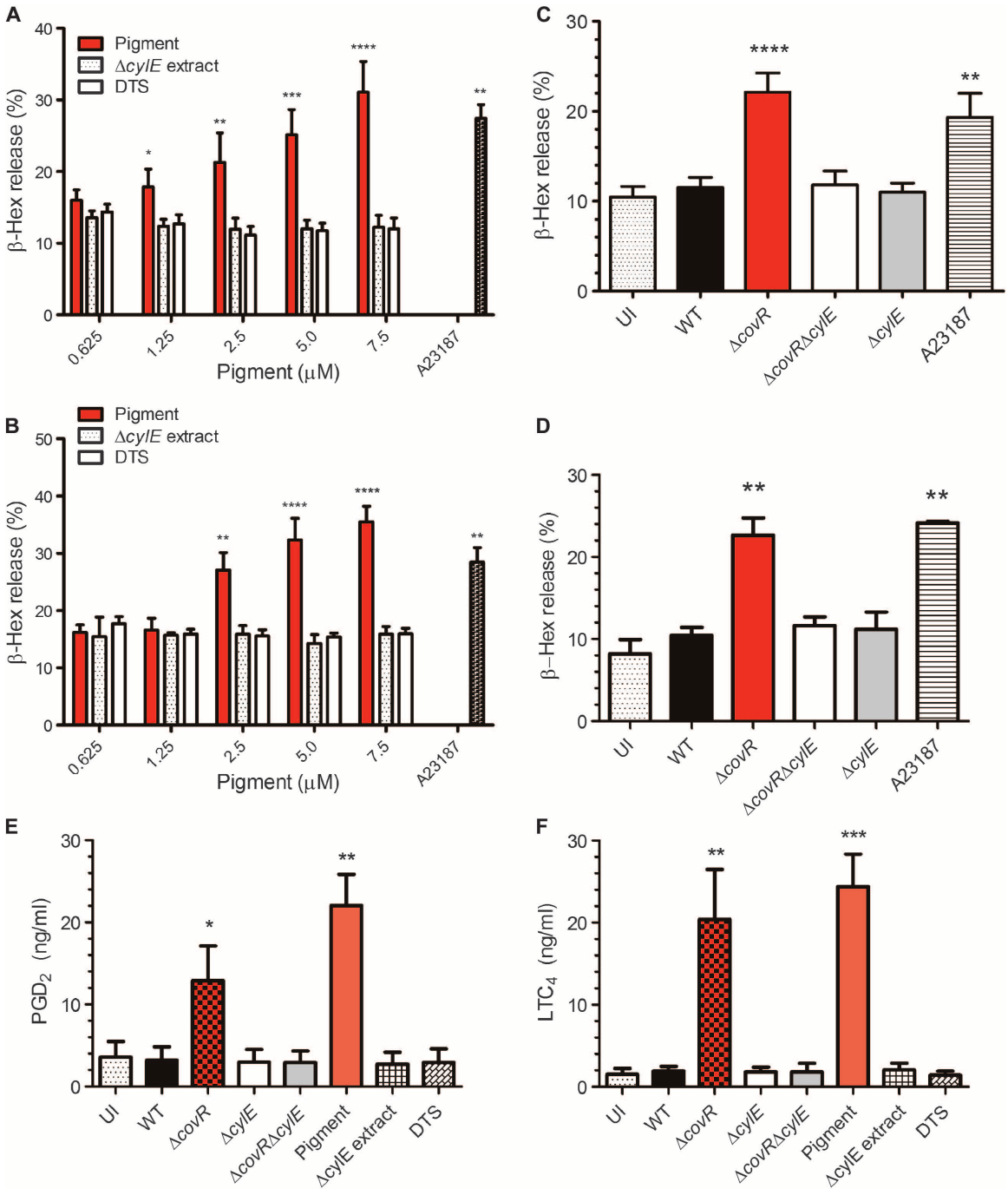

Fig. 1. The hemolytic pigment of GBS triggers the release of preformed mediators from mast cells. (**A** and **B**) About 10^5 BMCMCs (A) or PCMCs (B) were treated with varying amounts of the GBS pigment (0.625 to 7.5 μM). As controls, equal amounts of extract from the nonpigmented Δ*cylE* strain or DTS buffer were included. The Ca^{2+} ionophore A23187 (5 μM) was included as a positive control for mast cell degranulation. β-Hex release was measured 1 hour after treatment. Data shown were obtained from three independent experiments performed in duplicate with three independent batches of purified pigment [$n = 3$; *$P < 0.05$, **$P < 0.01$, ***$P < 0.001$, ****$P < 0.0001$, Bonferroni's multiple comparison test following analysis of variance (ANOVA); error bars, ±SEM]. (**C** and **D**) BMCMCs (C) or PCMCs (D) were exposed to either wild-type (WT) GBS A909, hyperhemolytic Δ*covR*, or nonhemolytic Δ*covR*Δ*cylE* or Δ*cylE* strains. Uninfected mast cells (UI) and mast cells treated with the Ca^{2+} ionophore A23187 (5 μM) were included as controls. β-Hex release was measured 1 hour after infection. Data shown were obtained from three independent experiments performed in duplicate ($n = 3$; **$P < 0.01$, ****$P < 0.0001$, Bonferroni's multiple comparison test following ANOVA; error bars, ±SEM). (**E** and **F**) PCMCs were exposed to either 0.625 μM pigment or controls (Δ*cylE* extract or DTS buffer) or the GBS strains indicated earlier for a period of 30 min. Release of PGD_2 and LTC_4 was measured. Data shown were obtained from four independent experiments ($n = 4$; *$P < 0.05$, **$P < 0.01$, ***$P < 0.001$, Bonferroni's multiple comparison test following ANOVA; error bars, ±SEM).

GBS strains with increased hemolytic pigment expression trigger mast cell degranulation.

Mast cell activation is also associated with the release of lipid-derived eicosanoids such as PGD_2 and LTC_4. Therefore, we examined if the GBS pigment and hyperhemolytic GBS induce the release of PGD_2 and LTC_4. The results shown in Fig. 1, E and F, indicate that both purified hemolytic pigment and hyperhemolytic GBSΔ*covR* induced PCMCs to release PGD_2 and LTC_4. Release of LTC_4 and PGD_2 was not observed in PCMCs that were treated with the nonhemolytic pigment (fig. S5, A and C) or when the primary antibody was omitted in the LTC_4 and PGD_2 assays of mast cells treated with hemolytic pigment (data not shown). Also, hyperpigmented GBS such as wild-type NCTC10/84 induced the release of LTC_4 and PGD_2 from mast cells, unlike the isogenic nonpigmented control NCTC10/84Δ*cylE* (fig. S5, B and D).

We further observed that mast cells released cytokines such as TNF and IL-6 when exposed to hyperpigmented GBSΔ*covR* or purified pigment (fig. S6). The amount of cytokine released from mast cells is similar to that observed when mast cells were activated by either lipopolysaccharide from *Escherichia coli* or peptidoglycan from *Staphylococcus aureus* (*29*). Of note, our previous studies have also confirmed that background absorbance from the GBS pigment does not contribute to significant values in cytokine assays (*17*). Collectively, these results indicate that both the purified pigment and hyperpigmented GBS strains trigger mast cell degranulation, resulting in the release of preformed and proinflammatory mediators.

Mast cell degranulation by the GBS pigment requires Ca^{2+} influx

We were next interested in understanding the mechanism of mast cell degranulation by the GBS pigment. Because calcium influx has been described to be important for mast cell degranulation (*30*–*32*), we tested the possibility that the GBS pigment induces the influx of Ca^{2+} into mast cells. To this end, PCMCs were pretreated with the fluorescent Ca^{2+} indicator (Fluo-4-AM) and exposed to either the GBS pigment (0.5 μM) or an equivalent amount of control Δ*cylE* extract or 5 μM A23187, and fluorescence was measured for a period of 15 min. Whereas Ca^{2+} influx was not observed in mast cells exposed to the control Δ*cylE* extract, the GBS pigment induced Ca^{2+} influx into mast cells, similar to the Ca^{2+} ionophore A23187 (Fig. 2A).

To determine if Ca^{2+} influx is essential for pigment-mediated mast cell degranulation, we exposed PCMCs to EGTA (Ca^{2+} chelator) before treatment with the GBS pigment or control Δ*cylE* extract. The results shown in Fig. 2B indicate that pretreatment of mast cells with EGTA significantly decreased the GBS pigment–mediated release of β-hex, similar to the control Ca^{2+} ionophore A23187. These results indicate that Ca^{2+} influx is important for GBS pigment–mediated mast cell degranulation. Previous studies have also indicated that activation of phosphatidylinositol 3-kinase (PI3K) or G protein (heterotrimeric guanine nucleotide–binding protein)–coupled receptors (GPCRs) can stimulate mast cell degranulation (*33*, *34*). To test if the GBS pigment used either PI3K or GPCR activation for mast cell degranulation, we exposed PCMCs to either LY294002 (PI3K inhibitor) or pertussis toxin (inhibitor of GPCRs) before treatment with the GBS pigment or control Δ*cylE* extract. We observed that pretreatment of mast cells with LY294002 or pertussis toxin did not significantly inhibit the pigment-mediated release of β-hex (Fig. 2B). Collectively, these results suggest that GBS pigment–mediated mast cell degranulation is dependent on Ca^{2+} influx but is independent of PI3K or GPCR activation.

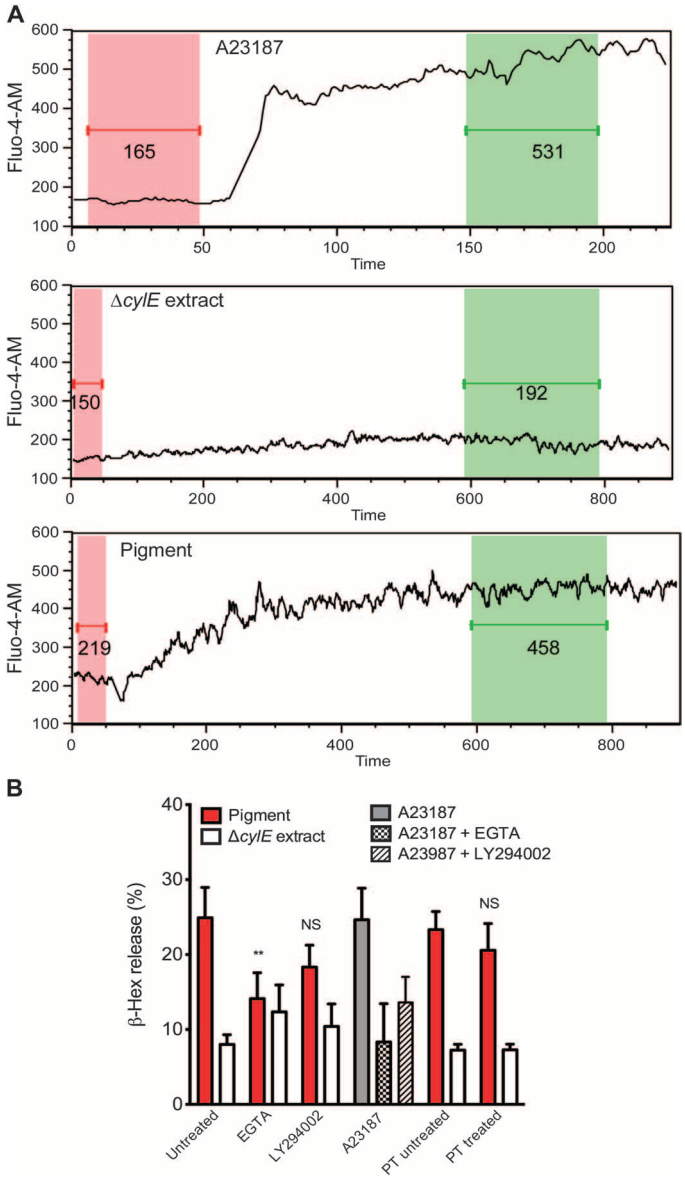

Fig. 2. Mast cell degranulation by the GBS pigment requires Ca^{2+} influx. (**A**) PCMCs were pretreated with the calcium indicator Fluo-4-AM, and calcium influx was recorded by flow cytometry. At 60 s, either 5 μM A23187 (top panel), 0.5 μM GBS pigment (bottom panel), or an equivalent amount of control Δ*cylE* extract (middle panel) was added. Mean fluorescence intensities of mast cells before treatment (red) and after treatment (green) are shown. Time is given in seconds. A representative image from one of three independent experiments is shown. (**B**) PCMCs were pretreated with either EGTA (4 mM) or LY294002 (100 μM) for 30 min or with pertussis toxin (PT; 200 ng/ml) for 2 hours. Untreated PCMCs were included as controls for both pretreatment conditions. Subsequently, the mast cells were exposed to either 2.5 μM pigment or an equivalent amount of Δ*cylE* extract or 5 μM A23187 for 1 hour. Release of β-hex was then quantified in the mast cell supernatants. Data shown were obtained from three independent experiments performed in duplicate and compared to the respective untreated mast cells (n = 3; $^{**}P$ = 0.002, Dunnett's multiple comparison test following ANOVA; error bars, ±SEM).

Mast cell degranulation by the GBS pigment contributes to cytotoxicity

Mast cell secretagogues such as mastoparan have been shown to trigger mast cell degranulation through activation of GPCRs, which subsequently leads to membrane permeabilization and mast cell death (*35*). Our above-mentioned results indicate that the GBS pigment induces mast cell degranulation independent of GPCR activation. We recently showed that GBS pigment induces membrane perturbations in artificial lipid bilayers and macrophages (*17*). Therefore, we hypothesized that the Ca^{2+} influx observed in mast cells is likely initiated by pigment-induced membrane perturbations. To test this hypothesis, mast cells (PCMCs) were exposed to GBS pigment (2.5 μM) or controls (Δ*cylE* extract or A23187), and the uptake of a membrane impermeable dye propidium iodide (PI) was measured over time (900 s or 15 min). The results shown in Fig. 3A indicate that increased fluorescence due to PI uptake is seen in mast cells exposed to the GBS pigment but not in mast cells treated with the Δ*cylE* extract. Although the GBS pigment triggered membrane permeability in mast cells within 900 s (15 min), a significant release of β-hex was observed between 30 and 60 min (fig. S7). These results suggest that the GBS pigment induces membrane permeability, which triggers Ca^{2+} influx, leading to mast cell degranulation and the release of mediators.

Scanning electron microscopy was also performed on mast cells that were exposed to the GBS pigment. As controls, mast cells were exposed to an equivalent amount of Δ*cylE* extract. The results shown in Fig. 3B indicate that mast cells treated with the GBS pigment exhibit morphological changes indicative of degranulation similar to mast cells treated with the Ca^{2+} ionophore A23187, but not with mast cells exposed only to medium or the Δ*cylE* extract. These data further confirm that the GBS pigment triggers mast cell degranulation.

To determine if mast cell degranulation induced by the GBS pigment can contribute to cytotoxic effects, we compared the release of the cytosolic enzyme LDH in pigment-treated mast cells where degranulation was inhibited by EGTA. To this end, PCMCs were pretreated with EGTA before treatment with the GBS pigment or control Δ*cylE* extract. As additional controls, we included mast cells pretreated with either LY294002 or pertussis toxin. The results shown in Fig. 3C indicate that inhibition of mast cell degranulation by EGTA significantly decreased, but did not abolish, the release of LDH. As expected, no significant inhibition in LDH release was observed in mast cells pretreated with LY294002 or pertussis toxin (Fig. 3C), similar to the lack of inhibition of β-hex by these compounds (Fig. 2B). LDH release from mast cells was also observed with increasing pigment concentrations and hyperpigmented GBS strains (fig. S8). Together, our results suggest that the GBS pigment induces membrane perturbations in mast cells, leading to Ca^{2+} influx and mast cell degranulation, which further contributes to the release of cytosolic components and mast cell death.

Hyperpigmented GBS strains induce rapid mast cell degranulation in vivo

We next hypothesized that increased expression of the pigment may induce mast cell degranulation in vivo, early during GBS infection. To test this hypothesis, we intraperitoneally injected wild-type (C57BL6/J) mice with ~ 10^7 CFU of GBS (wild type, Δ*covR*, or Δ*covR*Δ*cylE*) or control phosphate-buffered saline (PBS) (n = 6 per group). At 2 hours after inoculation, peritoneal lavage was performed, and mast cells present in the peritoneal fluid were stained as described (*25*, *26*). As shown in Fig. 4, A and B, extensive mast cell degranulation was observed in peritoneal fluid obtained from Δ*covR*-infected mice when compared to mice infected with the isogenic nonpigmented Δ*covR*Δ*cylE* strain or control PBS. Histamine levels were also significantly higher in plasma obtained from Δ*covR*-infected mice compared to mice infected with nonpigmented Δ*covR*Δ*cylE* (Fig. 4C). Similarly, hyperpigmented GBS strains such as wild-type GBS NCTC10/84 or GBSΔ*covS* induced mast cell degranulation during infection in vivo, unlike the isogenic nonpigmented controls, that is, NCTC10/84Δ*cylE* or Δ*covS*Δ*cyl*, respectively (figs. S9 and S10). Collectively, these results indicate that hyperhemolytic GBS strains induce mast cell degranulation in vivo.

Mast cell–deficient mice exhibit decreased inflammatory responses and neutrophil recruitment during systemic GBS infection

We previously showed that hyperpigmented GBS such as Δ*covR* are significantly more virulent in a murine model of systemic infection (*36*). Our above-mentioned results indicate that the hyperpigmented GBS activate mast cells both in vitro and in vivo. To determine if mast cells play a substantial role during systemic infection, we used a mouse strain that is deficient in mast cells [*Cpa3-Cre;Mcl-1*$^{fl/fl}$ (*37*)] and also included mast cell–proficient littermates as controls (*Cpa3-Cre;Mcl-1*$^{fl/+}$). The *Cpa3-Cre;Mcl-1*$^{fl/fl}$ mast cell–deficient mouse strain has been previously characterized, and these mice were shown to exhibit 92 to 100% deficiency in mast cells [for details, see (*37*)]. In our studies, we compared bacterial burden and inflammatory responses in mast cell–deficient mice [*Cpa3-Cre;Mcl-1*$^{fl/fl}$ (*37*)] and mast cell–proficient littermate controls (*Cpa3-Cre;Mcl-1*$^{fl/+}$) that were infected for 24 hours with the hyperpigmented GBSΔ*covR* or control nonpigmented GBSΔ*covR*Δ*cylE* strain (n = 7 per group).

Because GBS disseminate to the spleen during systemic infection (*36*, *38*), we compared bacterial burden and inflammatory responses in the spleens of infected mice. We observed that bacterial CFU were significantly higher in the spleens of mast cell–deficient mice than in the spleens of mast cell–proficient mice that were infected with Δ*covR* (Fig. 5A). The levels of cytokines such as TNF, IL-6, and KC (the murine functional homolog of IL-8) were significantly higher in the spleens of mast cell–proficient mice than in those of mast cell–deficient mice infected with GBSΔ*covR* (Fig. 5, B to D). Flow cytometric analysis indicated that the percentage of neutrophils ($Ly6G^+$ cells) was significantly increased in the spleens of mast cell–proficient mice when compared to those of mast cell–deficient mice (Fig. 5E). Also, bacterial CFU, cytokines/chemokines, and percent neutrophils were not significantly different between the spleens of mast cell–proficient and mast cell–deficient mice that were infected with Δ*covR*Δ*cylE* (Fig. 5, B to E). Histamine levels were higher in the blood of mast cell–proficient mice infected with Δ*covR* when compared to the blood of mast cell–proficient mice infected with Δ*covR*Δ*cylE* (Fig. 5F). Similar trends of increased bacterial burden and decreased levels of TNF, neutrophils, and histamine were also seen in peritoneal fluids of mast cell–deficient mice compared to mast cell–proficient mice infected with GBSΔ*covR* (fig. S11). Whereas mast cell release of IL-4 was indicated to dampen macrophage phagocytosis and aggravate sepsis (*15*), we did not observe significant differences in IL-4 levels in either the peritoneal fluid or spleens of mast cell–proficient and mast cell–deficient mice infected with GBS at 24 hours after infection (figs. S11 and S12).

The mast cell–deficient mice used in our studies (*Cpa3-Cre;Mcl-1*$^{fl/fl}$) have also been described to exhibit deficiencies in basophils [58 to 78% (*37*)]. To determine if basophil activation also played a critical role during

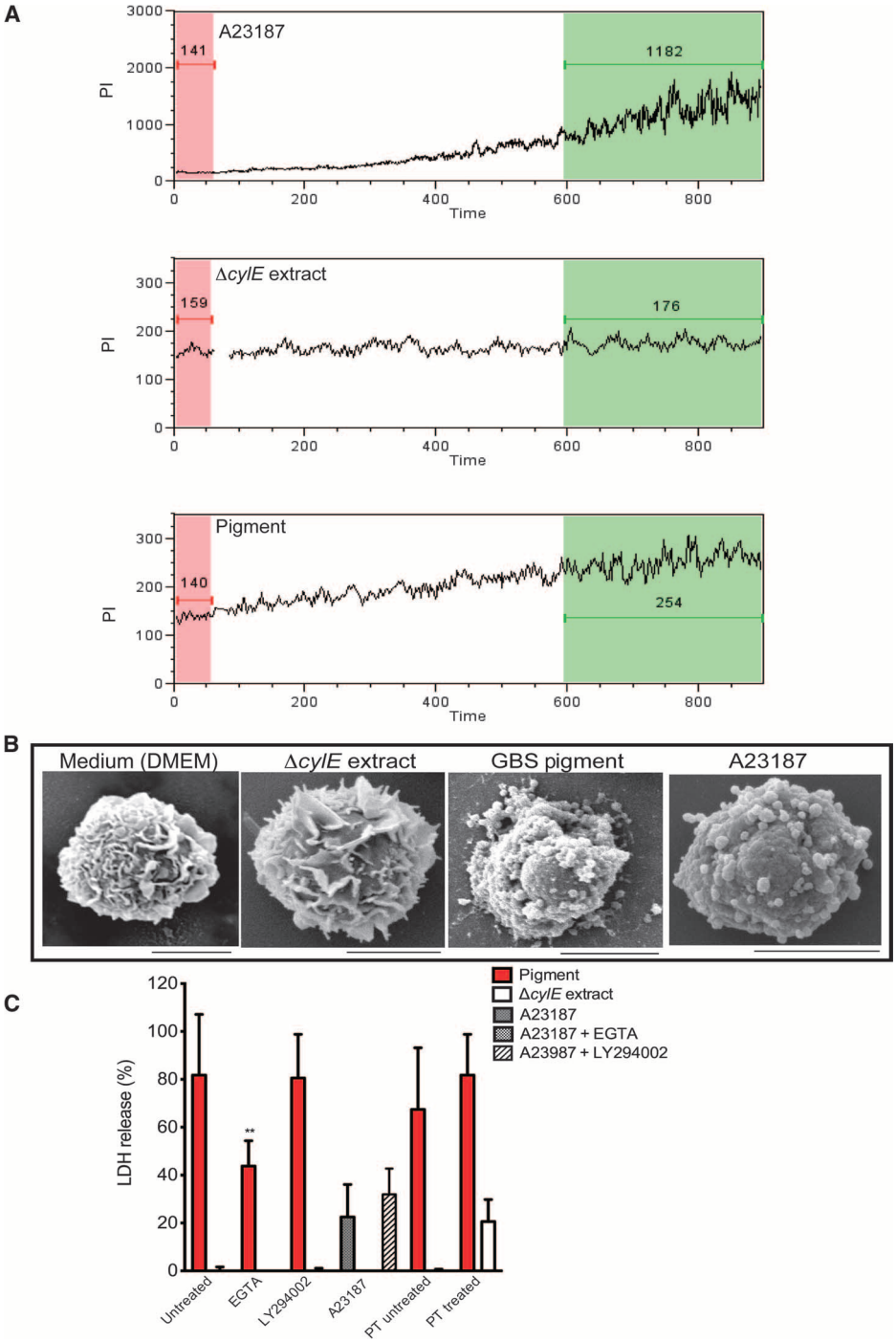

Fig. 3. Mast cell degranulation by the GBS pigment contributes to cytotoxicity. (**A**) PCMCs were pretreated with the membrane impermeable dye PI and then exposed to either 5 μM A23187 (top panel), 2.5 μM GBS pigment (bottom panel), or an equivalent amount of Δ*cylE* extract (middle panel). PI influx was recorded by flow cytometry, and time is given in seconds. Mean fluorescence intensities of mast cells before treatment (red) and after treatment (green) are shown. A representative image from one of two independent experiments is shown. (**B**) Scanning electron micrographs showing mast cells that were briefly exposed to 0.5 μM pigment or controls (cell culture medium, Δ*cylE* extract, or 1.66 μM A23187). A representative image from two independent experiments is shown. A minimum of 30 cells were examined in a blinded fashion. (**C**) PCMCs were pretreated with either EGTA (4 mM) or LY294002 (100 μM) for 30 min or with pertussis toxin (PT; 200 ng/ml) for 2 hours. Untreated PCMCs were included as controls for both pretreatments. Subsequently, the mast cells were exposed to either 2.5 μM pigment or an equivalent amount of Δ*cylE* extract or 5 μM A23187 for 1 hour. Release of the cytosolic enzyme lactate dehydrogenase (LDH) was measured in the mast cell supernatants. Data shown were obtained from three independent experiments performed in duplicate ($n = 3$; $^{**}P = 0.006$, Tukey's multiple comparison test following ANOVA; error bars, ±SEM).

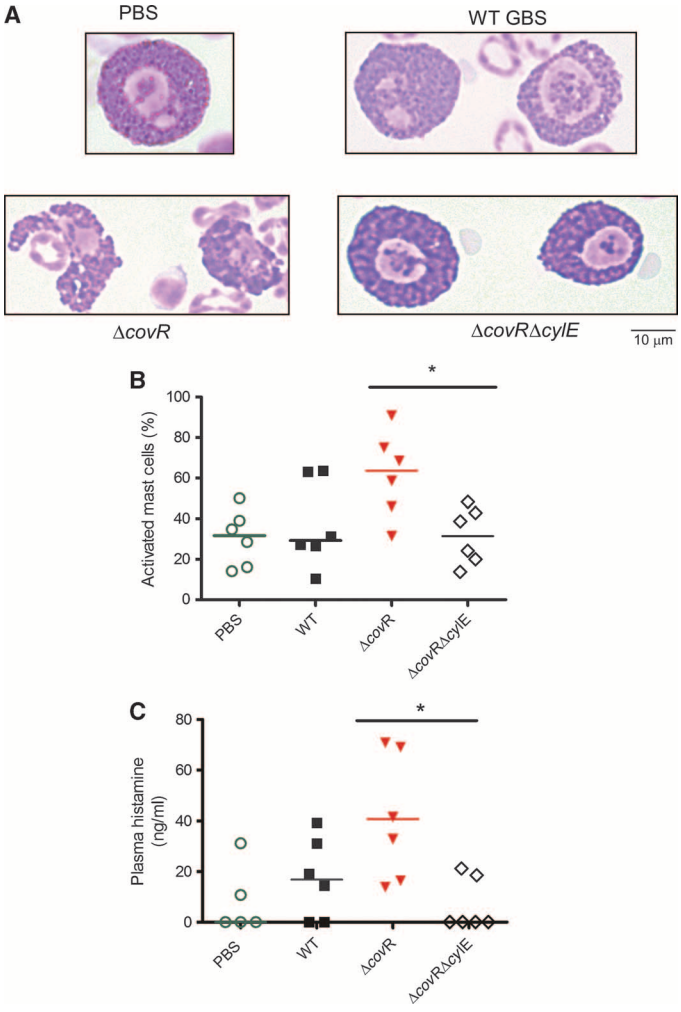

Fig. 4. Hyperpigmented GBS strains induce rapid mast cell degranulation in vivo. WT C57BL6/J mice (n = 6 per group) were infected intraperitoneally with 10^7 CFU of either WT GBS or isogenic Δ*covR* or Δ*covR*Δ*cylE* strains. Peritoneal fluid and blood were collected 2 hours after infection. Data shown are representative of two independent experiments. (**A** and **B**) Peritoneal cells were cytocentrifuged and stained with May-Grünwald-Giemsa. A representative image showing intact (PBS) and activated mast cells (Δ*covR*) is shown. Activated mast cells in peritoneal fluid were scored in a blinded fashion, and percent activated mast cells was calculated as the number of activated mast cells divided by the total number of mast cells in randomly selected fields × 100 (n = 30 cells per group; *P < 0.05, Bonferroni's multiple comparison test following ANOVA; medians are shown). (**C**) Histamine levels were measured in the plasma isolated from the blood of mice infected with the GBS strains indicated earlier (n = 6 per group; *P < 0.05, Bonferroni's multiple comparison test following ANOVA; medians are shown).

systemic infection with hyperpigmented GBSΔ*covR*, we compared bacterial burden, cytokine responses, and histamine release in the spleens and peritoneal fluid of basophil-depleted mice [$Mcpt8^{DTR}$ (*39*)] and control wild-type (C57BL6/J) mice that were infected with GBSΔ*covR*. The results shown in fig. S13 indicate that the presence or absence of basophils did not significantly alter bacterial burden in either the spleens or peritoneal fluid. Moreover, the levels of histamine or cytokines TNF, IL-6, KC, and IL-4 were not significantly different between wild-type and basophil-depleted mice infected with GBSΔ*covR* (fig. S13). Also, no significant difference was observed in the levels of TNF, IL-6, KC, and IL-4 in the peritoneal fluid of wild-type and basophil-depleted mice infected with GBSΔ*covR*. Collectively, these results suggest that mast cell activation promotes the induction of a proinflammatory response to decrease systemic GBS infection.

Activation of mast cells decreases GBS vaginal colonization

We next examined the role of mast cells in GBS vaginal colonization. Similar to humans, mast cells are present in high numbers in the lower genital tract of mice (*6*, *40*). We previously observed that when compared to wild-type or nonhemolytic/nonpigmented GBS, hyperpigmented GBSΔ*covR* showed decreased ability to colonize the lower genital tract of mice between 2 and 5 days after inoculation (*41*). Our above-mentioned results indicate that the hyperpigmented GBS strain activates mast cells. Thus, we hypothesized that if mast cell activation prevents colonization of hyperpigmented GBS, then these GBS strains may exhibit increased persistence in the vaginal tracts of mast cell–deficient mice. To test this hypothesis, 12- to 16-week-old female mast cell–deficient mice (*Cpa3-Cre;Mcl-1*$^{fl/fl}$) and littermate control mast cell–proficient mice (*Cpa3-Cre;Mcl-1*$^{fl/+}$) were inoculated with saline or ~1×10^8 to 5×10^8 CFU of hyperpigmented GBSΔ*covR* or isogenic, nonpigmented GBSΔ*covR*Δ*cylE* in the vaginal lumen (n = 8 per group). At 4 days after inoculation, reproductive tracts were excised from the euthanized mice, and GBS CFU was enumerated in the lower genital tract and uterine horns (for details, see Materials and Methods). The results shown in Fig. 6, A to C, indicate that hyperpigmented GBSΔ*covR* was cleared more frequently from the lower genital tract and uterine horns of mast cell–proficient mice when compared to mast cell–deficient mice. In contrast, the nonpigmented GBSΔ*covR*Δ*cylE* strain showed increased persistence in mast cell–proficient mice when compared to GBSΔ*covR* (Fig. 6, A to C). Also, the persistence of GBSΔ*covR*Δ*cylE* was not significantly different between mast cell–proficient and mast cell–deficient mice (Fig. 6, A to C). Consistent with these observations, histamine levels were significantly greater in the genital tracts of mast cell–proficient mice compared to mast cell–deficient mice that were inoculated with hyperpigmented GBSΔ*covR* (Fig. 6D). Histamine levels were not significantly different between mast cell–proficient and mast cell–deficient mice infected with the nonpigmented GBSΔ*covR*Δ*cylE* strain (Fig. 6D). Toluidine blue staining of histological sections of the mouse genital tract revealed the presence of nondegranulated mast cells in mast cell–proficient mice that were treated with control PBS or nonpigmented GBSΔ*covR*Δ*cylE* (Fig. 7A, panels i and iii), whereas degranulated mast cells are seen in mast cell–proficient mice infected with hyperpigmented GBSΔ*covR* (Fig. 7A, panel ii). As expected, mast cells were not observed anywhere in the lower genital tract of mast cell–deficient mice (for representative sections, see Fig. 7A, panels iv to vi). Hematoxylin and eosin (H&E) staining of histological sections of the genital tract revealed the presence of inflammatory foci in mast cell–proficient mice that were infected with hyperpigmented GBSΔ*covR* (Fig. 7B, panel ii) but not in mast cell–proficient mice infected with GBSΔ*covR*Δ*cylE* or treated with PBS (Fig. 7B, panels i and iii). Inflammatory foci were not observed in the lower genital tracts of mast cell–deficient mice infected with GBSΔ*covR*, GBSΔ*covR*Δ*cylE*, or control PBS (Fig. 7B, panels iv to vii). Also, the lower genital tract of mast cell–deficient mice treated with PBS did not exhibit signs of inflammation (Fig. 7B, panel iv), suggesting the lack of compensatory alterations

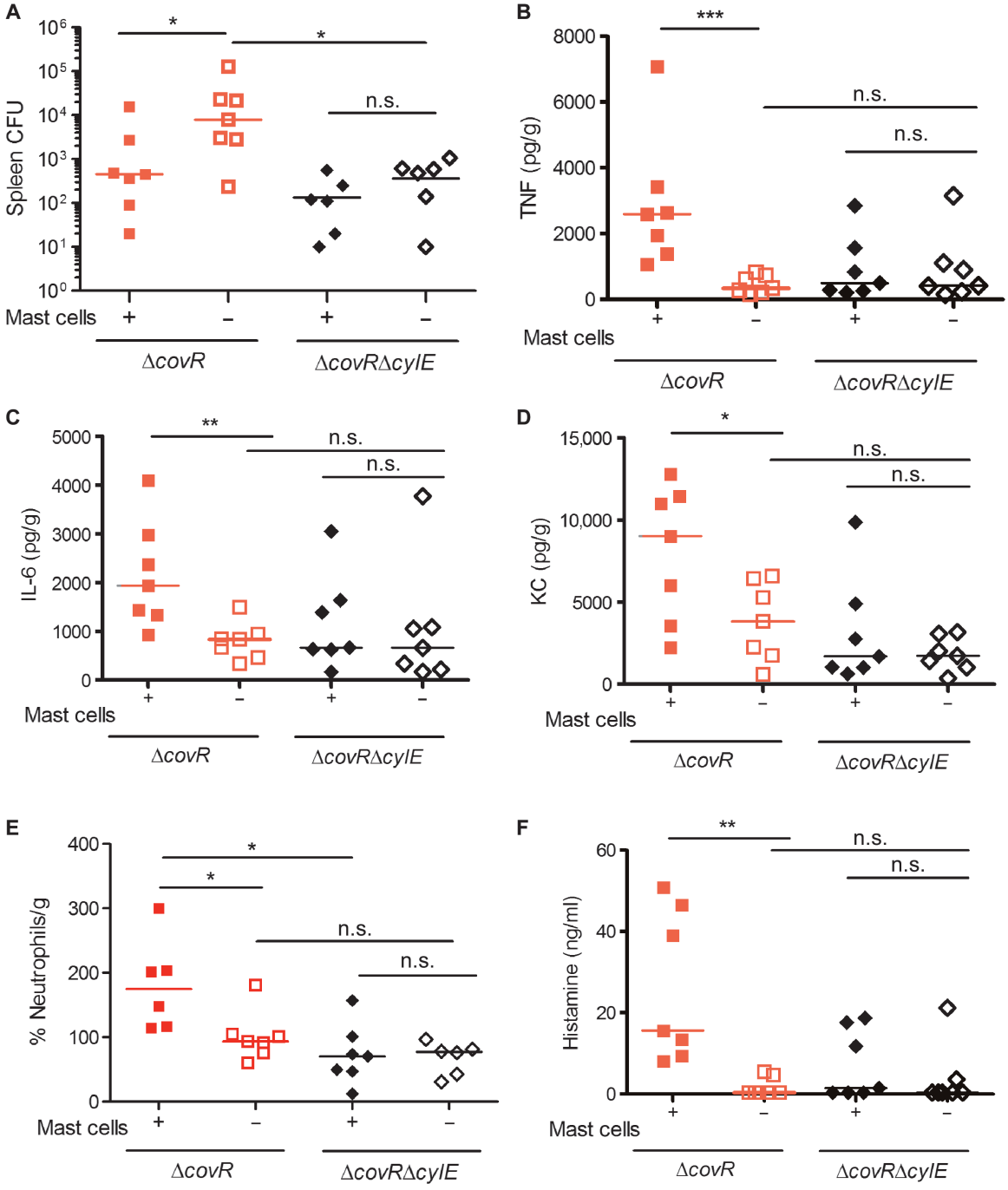

Fig. 5. Mast cell–deficient mice exhibit impaired bacterial clearance and reduced levels of proinflammatory cytokines and neutrophils during systemic GBS infection. Mast cell–deficient mice and mast cell–proficient littermate controls were infected intraperitoneally with hyperhemolytic/hyperpigmented GBS*ΔcovR* and control nonhemolytic/nonpigmented *ΔcovRΔcylE*. At 24 hours after infection, bacterial burden, inflammatory cytokines, and neutrophil levels were evaluated. Data shown are from a representative experiment of two independent experiments containing seven animals per group. The Mann-Whitney test was used for comparison between two groups, and Bonferroni's multiple comparison test following ANOVA was used for multiple comparisons. Medians are indicated. (**A**) Bacterial burden in the spleens of mast cell–proficient and mast cell–deficient mice infected with GBS*ΔcovR* and *ΔcovRΔcylE* [*$P < 0.05$; n.s. (not significant), $P > 0.4$]. (**B** to **D**) Cytokine TNF, IL-6, and KC levels in the spleens of mast cell–proficient and mast cell–deficient mice infected with GBS*ΔcovR* and *ΔcovRΔcylE* (*$P < 0.05$; **$P < 0.01$; ***$P < 0.005$; n.s., $P > 0.1$). (**E**) Percent neutrophils ($Ly6G^+$ $CD11b^+$ cells) in the spleens of mast cell–proficient and mast cell–deficient mice infected with GBS*ΔcovR* (*$P < 0.05$). (**F**) Histamine levels in the plasma isolated from mast cell–proficient and mast cell–deficient mice infected with GBS*ΔcovR* and *ΔcovRΔcylE* (*$P < 0.05$).

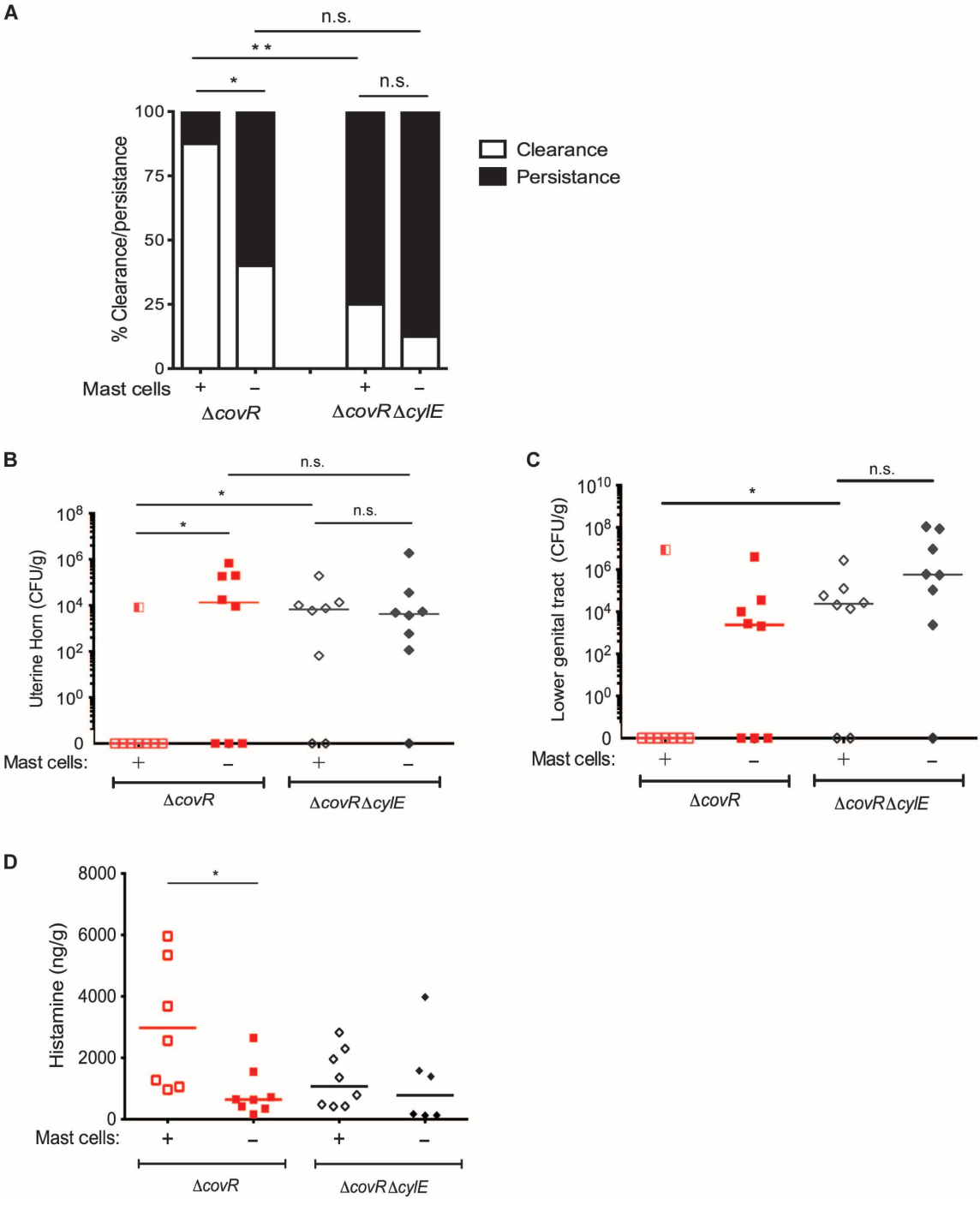

Fig. 6. Mast cell activation promotes clearance of hyperhemolytic GBS from the lower genital tract. Mast cell–deficient mice or heterozygous littermate controls were intravaginally inoculated with ~10^8 CFU of GBS Δ*covR* or Δ*covR*Δ*cylE*. At 4 days after inoculation, bacterial persistence and dissemination were evaluated in the lower genital tract and both uterine horns. (**A**) Data shown are from an experiment containing eight animals per group. Barnard's test was used to estimate differences in percent clearance/persistence. (**B** to **D**) The Mann-Whitney test was used for comparison between two groups, or Bonferroni's multiple comparison test following ANOVA was used for multiple comparisons. (A) Negative or positive bacterial cultures obtained from the lower genital tract and both uterine horns of mast cell–proficient mice and mast cell–deficient mice that were inoculated with either GBSΔ*covR* or Δ*covR*Δ*cylE*. Data are represented as percent clearance compared to persistence (n = 8 per group; *P = 0.028, **P = 0.007, Barnard's test). (B) Bacterial burden in the uterine horns and lower genital tract of mast cell–proficient and mast cell–deficient mice infected with GBS Δ*covR* or Δ*covR*Δ*cylE* (n = 8 per group; *P < 0.05). In the mast cell–proficient group inoculated with GBSΔ*covR*, the same mouse had bacterial CFU in both the lower genital tract and uterine horns (denoted as a partially filled symbol). (C) Histamine levels in the genital tract of mast cell–proficient and mast cell–deficient mice infected with GBSΔ*covR* or Δ*covR*Δ*cylE* (n = 8 per group; *P < 0.05).

in the myeloid lineage in the lower genital tracts of these mice. Together, these results indicate that mast cells play a role in clearance of hyperpigmented GBS strains from the lower genital tract.

Similar to our observations with Δ*covR*, we observed that vaginal colonization of natively hyperpigmented wild-type NCTC10/84 was significantly lower than that of the isogenic nonpigmented NCTC10/84Δ*cylE* (fig. S14A). Degranulating mast cells were seen in toluidine blue–stained histological sections of the lower genital tracts of mice infected with NCTC10/84, and nondegranulating mast cells were observed in NCTC10/84Δ*cylE* (fig. S14B, panels i and ii and magnified insets). H&E-stained sections revealed the presence of edema in mice infected with NCTC10/84 (panel iii) but not in mice infected with NCTC10/84Δ*cylE* (panel iv).

Together, our studies suggest a potential role for mast cells in limiting genital colonization by hyperpigmented/hyperpathogenic GBS. The role of mast cells in the prevention of GBS infections has important implications for strategies that can decrease the risk of infection-associated preterm births and early-onset neonatal infections.

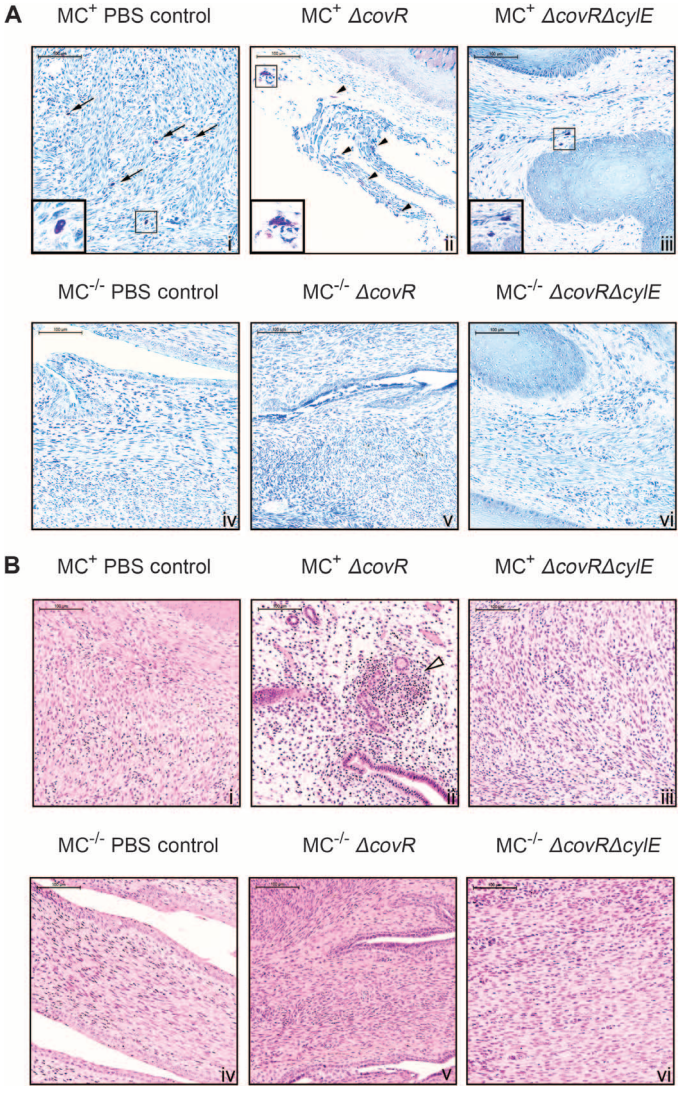

Fig. 7. Histological sections of the genital tracts of female mast cell–proficient and mast cell–deficient mice infected with hyperpigmented and nonpigmented GBS strains. Histology of mouse genital tracts at 4 days after inoculation with GBS (Δ*covR* or Δ*covR*Δ*cylE*) or control PBS. (**A**) Toluidine blue–stained sections. Mast cells were not observed in the lower genital tracts of mast cell–deficient ($MC^{-/-}$) mice (panel iv to vi). (**B**) H&E-stained sections. (A) Arrows and boxed area indicate nondegranulated mast cells in mast cell–proficient (MC^{+}) mice treated with control PBS or GBSΔ*covR*Δ*cylE* (panels i and iii and magnified insets). In mast cell–proficient mice treated with GBSΔ*covR*, arrowheads indicate degranulated mast cells (panel ii and magnified inset). (B) H&E-stained sections of mouse genital tracts reveals the presence of inflammatory foci in mast cell–proficient mice infected with GBSΔ*covR* (arrowhead in panel ii) in contrast to mast cell–proficient mice treated with PBS or GBSΔ*covR*Δ*cylE* (panels i and iii). Inflammatory foci are also absent in mast cell–deficient ($MC^{-/-}$) mice treated with PBS, GBSΔ*covR*, or GBSΔ*covR*Δ*cylE* (panels iv to vi). Scale bars, 100 μm.

DISCUSSION

Infection-associated preterm birth is thought to begin with microbial trafficking from the lower genital tract into the uterus (*42*). Although GBS frequently exists as a commensal organism in the lower genital tract of humans, not much is known about host immune surveillance that prevents ascending infection during pregnancy. Here, we examined how mast cells respond to GBS colonization and systemic infection. In contrast to the well-known detrimental role of mast cells during IgE-associated allergic responses like asthma, the role of mast cells as "initiators" of the proinflammatory response against invading pathogens has been considered to be beneficial to the host. Whereas the role of mast cells in the lower genital tract is not understood, an increased abundance of mast cells was observed in endocervical smears associated with *Trichomonas vaginalis* cervicitis (*43*). Also, mast cell numbers have been reported to increase in the vagina and cervix during pregnancy and labor (*44*). Our work is the first to suggest that mast cell activation in the lower genital tract may function as a mechanism of host immune surveillance.

Here, we demonstrate that the GBS hemolytic pigment degranulates mast cells. Both the purified hemolytic pigment and hyperpigmented GBS strains triggered the release of preformed and proinflammatory mediators from PCMCs and BMCMCs. The increase in uptake of the membrane impermeable dye PI, as well as the requirement for Ca^{2+}, suggests that the GBS hemolytic pigment induces membrane perturbations in mast cells, triggering Ca^{2+} influx and mast cell degranulation, which in part contribute to mast cell cytotoxicity similar to IgE-independent secretagogues such as mastoparan (*45*–*47*). However, in contrast to mastoparan, GBS pigment–mediated degranulation is independent of G protein activation. The amount of pigment required for mast cell degranulation (>0.5 μM) is significantly higher than the effective concentration 50 (EC_{50}) required for hemolysis [0.11 μM (*16*)], suggesting that mast cell degranulation by GBS occurs when pigment production is increased such as with hyperhemolytic/hyperpigmented strains. Consistent with these in vitro observations, we observed that systemic infection with hyperpigmented GBS rapidly induced mast cell degranulation in wild-type mice. Furthermore, when compared to mast cell–proficient mice, mast cell–deficient mice exhibit increased bacterial burden and diminished cytokine responses and neutrophil mobilization to the spleens during GBS systemic infection. Histamine release was observed in wild-type but not in mast cell–deficient mice, suggesting that mast cells are likely to be the primary source of histamine during systemic GBS infection. Whereas basophils also release histamine and other proinflammatory mediators (*48*), our results comparing wild-type

and basophil-depleted mice indicated no significant difference in GBS CFU, cytokine recruitment, or histamine release during systemic GBS infection. These data indicate that mast cells are critical for the proinflammatory response observed during systemic infection with hyperpigmented GBS strains.

The presence of hyperpigmented GBS in the lower genital tract also diminished bacterial vaginal colonization in wild-type but not in mast cell–deficient mice. Activation of mast cells in the lower genital tract was confirmed histologically and correlated with histamine release. In contrast to our observations, a previous report indicated that no significant difference was observed in vaginal colonization of natively occurring hyperpigmented GBS such as NCTC10/84 when compared to its isogenic nonpigmented control in a mono-infection model (*49*). We speculate that the use of 17β-estradiol to synchronize mice for estrus in these previous studies (*49*) and its effect on mast cell activation (*50*) may, in part, have contributed to the disparate results compared to our study. Whereas we previously described the role of neutrophils in GBS vaginal colonization (*41*), our studies here demonstrate that mast cells, which are sentinel immune cells, are likely the primary initiators of the proinflammatory response against hyperpigmented/hyperpathogenic GBS.

The mast cell–dependent proinflammatory response due to hyperpigmented GBS also resulted in diminished recovery of commensal bacteria from the lower genital tract. We observed that mast cell–proficient mice that cleared hyperpigmented GBS from their lower genital tracts also had fewer commensal organisms (0 to 10^2 commensals/g tissue). In comparison, we observed that $>10^5$ to 10^7 commensals/g tissue were present in mast cell–deficient mice inoculated with hyperpigmented GBS. Also, $>10^5$ to 10^7 commensals/g tissue were present in untreated mice or mice inoculated with nonpigmented GBS. Together, our studies indicate that the threshold for mast cell degranulation by the GBS hemolytic pigment is greater than what is normally expressed by weakly hemolytic wild-type GBS strains (for example, A909 or COH1). We predict that this high threshold for mast cell degranulation likely minimizes unnecessary inflammatory responses that can otherwise have a detrimental effect on the existence of beneficial commensal organisms in the vaginal tract as suggested (*51*–*54*).

Previous studies have shown that expression of the GBS pigment is controlled by the pH-responsive CovR/S system (*55*). Thus, repression of the hemolytic pigment at lower pH (*55*) such as the acidic pH of the vagina (pH 4 to 5) likely prevents mast cell activation and favors the existence of GBS as a commensal. Owing to limitations in the numbers of mast cell–deficient mice, we primarily used the genetically modified GBSΔ*covR* strain and its isogenic nonpigmented control GBSΔ*covR*Δ*cylE* to characterize the role of increased hemolytic pigment expression in an in vivo model. Nevertheless, we confirmed that mast cell activation by the GBS hemolytic pigment is recapitulated both in vitro and in vivo by natively occurring hyperpigmented GBS such as NCTC10/84 and even by the hyperpigmented GBSΔ*covS* strain, but not by isogenic nonpigmented controls. We predict that when hemolytic pigment expression is increased because of either changes in environmental conditions such as higher pH (*55*) or spontaneous mutations in CovR/S (*16*), the risk of ascending infection is greater, and mast cells can initially respond to this increase in danger signal. Exciting future avenues include understanding how specific mast cell mediators limit GBS colonization and infection.

Previous reports have indicated that mast cells are antimicrobial to pathogens such Group A *Streptococcus* through the action of a cathelicidin antimicrobial peptide (*56*). Mast cells also store a number of other antimicrobial factors such as proteases and other enzymes (*57*). However, we observed that mast cells did not adversely affect the growth of GBS in vitro (data not shown). Mast cell activation during microbial infection can have a beneficial or detrimental effect on the host, depending on the nature of infection and the type of mast cells that are activated. In contrast to the detrimental role of mast cell activation in host defense against *S. aureus* skin infections (*30*) and *Streptococcus pneumoniae* lung infection (*58*), we describe that mast cell activation by the GBS pigment/lipid toxin favored eradication of the pathogen from the lower genital tract.

Although there are no reports describing mast cell deficiency in humans, we speculate that ascending infection leading to the presence of hyperhemolytic GBS in the amniotic fluid and chorioamniotic membranes of women in preterm labor (*16*) may, in part, be due to diminished mast cell activation and/or subsequent initiation of a proinflammatory response that failed to eradicate the pathogen from the lower genital tract. A structural difference between skin mast cells of Caucasian and African Americans has been reported (*59*), which, if related to a difference in threshold for mast cell activation, may be another contributing factor to the higher incidence of preterm birth in African Americans (*60*, *61*).

In summary, we show that mast cells respond to the membrane damage induced by a bacterial lipid toxin by releasing proinflammatory mediators that decrease bacterial burden during GBS colonization and infection. For the first time, we describe the importance of mast cell activation as a host mechanism to decrease the burden of vaginal colonization by hypervirulent GBS.

MATERIALS AND METHODS

All chemicals were purchased from Sigma-Aldrich, unless mentioned otherwise. Cell culture medium was purchased from Corning CellGro or Mediatech Inc.

Human samples

GBS clinical isolates from rectovaginal swabs were obtained from women in their third trimester of pregnancy at the University of Washington Medical Center and Harborview Medical Center in 2007 under University of Washington Institutional Review Board (IRB) protocol #30308; samples were collected without any identifiers or clinical information, and a waiver for written informed consent was obtained for testing anonymous samples. Written informed patient consent for donation of human blood was obtained with approval from the Seattle Children's Research Institute IRB (protocol #11117).

Bacterial isolates

The wild-type GBS strains A909 and COH1 used in this study are clinical isolates obtained from infected human newborns (*62*, *63*). The Δ*cylE*, Δ*covR*, and Δ*covR*Δ*cylE* mutants were previously derived from A909 or COH1 (*16*, *20*, *36*). GBS lacking CovS (Δ*covS*) was previously derived from wild-type A909 (*16*). The plasmid pHY304Δ*cylX-K* (*16*) was used to derive a nonhemolytic/nonpigmented GBS strain in A909Δ*covS*, using previously described methods (*16*). The loss of hemolytic activity and pigment production in Δ*covS*Δ*cyl* is shown in fig. S3C. The previously described natively occurring hyperpigmented GBS strain NCTC10/84 (*23*) and its nonpigmented NCTC10/84Δ*cylE* control (*21*) were also used in this study. GBS were grown in tryptic soy

broth (TSB; Difco Laboratories) at 30° or 37°C in 5% CO_2. Cell growth was monitored at 600 nm.

Hemolytic titer estimation of GBS strains

To measure hemolytic activity from the various GBS isolates, hemolytic titer assays were performed as previously described (*64*) with a few modifications. TSB containing 1% glucose and 3% Tween 20 was inoculated with the GBS isolates and grown overnight at 30°C in a 96-well plate. Bacteria were pelleted, and the supernatants were transferred to a new plate. Twofold serial dilutions were performed in PBS, and a 1% suspension of human red blood cells (RBCs) was added at a ratio of 1:1. Cells were incubated for 1 hour at 37°C. Unlysed RBCs were pelleted by centrifugation, and hemoglobin release in the supernatant was measured as absorbance at 420 nm, using a plate reader (BioTek). Absorbances were normalized to control wells containing either PBS (0% lysis) or 0.1% SDS (100% lysis), and the reciprocal of the highest dilution giving at least 50% lysis was considered to be the hemolytic titer.

Purification of the GBS hemolytic pigment

The GBS hemolytic pigment was purified as previously described (*16*). Briefly, pigment was extracted from wild-type GBS A909 with DMSO/0.1% TFA, precipitated using NH_4OH, and column-purified using a Sephadex LH-20 (GE Healthcare) column as described (*16*). Fractions containing purified pigment were pooled, precipitated with NH_4OH, washed three times with high-performance liquid chromatography–grade water and then twice with DMSO, and lyophilized as described (*16*). The pigment extraction procedure was also performed in parallel on the nonpigmented strain GBSΔ*cylE*, and this extract was used as a control for pigment in all experiments, along with DTS buffer, which was used to resuspend pigment and control Δ*cylE* extract. Three independent pigment preparations were used in this study, and all preparations were confirmed to be hemolytic as described previously (*16*). Mass spectrometry and nuclear magnetic resonance were used to confirm the presence of pigment exclusively in the pigment samples and not in the control Δ*cylE* extract as shown previously (*16*).

Animal studies

All animal experiments were approved by the Seattle Children's Research Institutional Animal Care and Use Committee (protocols #13311 and #13907) and performed in strict accordance with the recommendations in the *Guide for the Care and Use of Laboratory Animals (Eighth Edition)*. All animal experiments were repeated twice unless mentioned otherwise.

Generation of BMCMCs

BMCMCs were isolated and cultured as previously described (*37*). Briefly, femoral bone marrow cells from wild-type C57BL6/J mice were cultured for 6 weeks in cell culture medium [Dulbecco's modified Eagle's medium (DMEM) + 10% fetal bovine serum (FBS) + 50 μM beta-mercaptoethanol (BME)] supplemented with IL-3 (10 ng/ml) to generate BMCMCs.

Generation of PCMCs

PCMCs were generated as previously described (*25*, *26*). Briefly, peritoneal cells from wild-type C57BL6/J mice were maintained in vitro for 2 to 4 weeks in medium (DMEM + 10% FBS + 50 μM BME) containing IL-3 (10 ng/ml) and stem cell factor (50 ng/ml) until mast cells represented >90% of the total nonadherent cells.

GBS activation of mast cells

About 10^5 BMCMCs or PCMCs were exposed to wild-type GBS A909 or isogenic Δ*cylE*, Δ*covR*, Δ*covR*Δ*cylE*, Δ*covS*, or Δ*covS*Δ*cyl* mutants, and mast cells were assessed for degranulation. Briefly, 10^7 CFU of the GBS strains indicated earlier were grown to an optical density at 600 nm (OD_{600}) of 0.3, washed, resuspended in PBS, and exposed to mast cells. The infection was carried out for a period of 1 hour, after which the release of β-hex and LDH was determined as indicated below. Controls included mast cells that were activated with 5 μM (2.5 ng/μl) of the Ca^{2+} ionophore A23187. All experiments were performed three independent times. The experiment was also repeated using natively hyperpigmented wild-type GBS NCTC10/84 and isogenic nonpigmented NCTC10/84Δ*cylE*.

Pigment activation of mast cells

BMCMCs or PCMCs were exposed to varying concentrations of purified pigment or controls [Δ*cylE* extract or DTS buffer; see (*16*)] for a period of 1 hour, after which the release of β-hex and LDH was determined as indicated below. Controls included mast cells that were activated with 5 μM (2.5 ng/μl) of the Ca^{2+} ionophore A23187. Additional controls included were mast cells that were treated with the nonhemolytic GBS pigment [that is, pigment lacking the carrier molecule starch (*17*)] and assays where the *p*-nitrophenyl-*N*-acetyl-β-D-glucosaminide (*p*-NAG) substrate was omitted (see below). All experiments were performed three independent times.

Measurement of mast cell activation/degranulation

The β-hex release assay was performed as previously described (*25*), using mast cells resuspended in Tyrode's buffer without bovine serum albumin (BSA). Briefly, β-hex release was quantified in mast cell supernatants and pellets, using an enzyme activity assay with *p*-NAG (Sigma-Aldrich) as the substrate. About 10 μl of mast cell supernatant or cell pellets that were lysed with Triton X-100 was treated with 50 μl of *p*-NAG solution (1.3 mg/ml) in 100 mM sodium citrate (pH 4.5) and incubated at 37°C for 1 hour. The reaction was stopped by the addition of 150 μl of 200 mM glycine (pH 10. 7), and the absorbance at 405 nm was measured. Percent β-hex release was calculated using the formula (absorbance$_{405}$ in mast cell supernatant)/(absorbance$_{405}$ in mast cell supernatant + absorbance$_{405}$ in mast cell pellet) × 100. Also, the *p*-NAG substrate was omitted in control assays performed with supernatant obtained from mast cells treated with hemolytic pigment to rule out potential pigment absorbance.

The PGD_2 and LTC_4 secretion assays were performed in DMEM. Briefly, 10^5 PCMCs were treated with either purified GBS pigment (0.625 μM), an equivalent amount of controls, or 10^7 CFU of GBS (either wild-type A909 or isogenic mutants Δ*cylE*, Δ*covR*, or Δ*covR*Δ*cylE*, or wild-type NCTC10/84 and isogenic NCTC10/84Δ*cylE*) for 30 min. PCMCs were then centrifuged, and the supernatant (~10 μl) was used to measure the release of PGD_2 and LTC_4, using the Prostaglandin D_2 EIA Kit and Leukotriene C_4 EIA Kit (Cayman Chemicals) as per the manufacturer's instructions. To exclude a potential interference of pigment absorbance, additional controls included were mast cells that were treated with the nonhemolytic pigment [lacking the carrier molecule starch (*17*)] and mast cells treated with hemolytic pigment but where the primary antibody to PGD_2 or LTC_4 was omitted in the assays.

LDH release in mast cell supernatants (10 μl) was determined using an LDH assay as per the manufacturer's (Clontech) instructions. Inflammatory cytokine release was measured by Luminex bead assays (eBioscience) using 50 μl of mast cell supernatants that were treated with

pigment, controls, or GBS for a period of 4 hours. All experiments were performed three independent times.

Calcium influx assay

Calcium influx assays were performed as described (*30*) with a few modifications. Briefly, 2×10^5 PCMCs were loaded with 5 μM of the fluorescent Ca^{2+} indicator (Fluo-4-AM, Life Technologies) for 30 min, and cells were then washed and resuspended in Tyrode's buffer without BSA. Fluorescence intensity was measured using flow cytometry (LSRII instrument, BD Biosciences). After an initial reading of 60 s, mast cells were exposed to either the GBS pigment (0.5 μM) or an equivalent amount of control Δ*cylE* extract or 5 μM A23187 and monitored for an additional 840 s (180 s for A23187). Data were collected using the FACSDiva software system (BD Biosciences) and analyzed by FlowJo (TreeStar).

Membrane permeabilization assay

To assess membrane permeabilization, uptake of the membrane impermeable dye PI (Life Technologies) was measured. Briefly, 2×10^5 PCMCs were loaded with 3.75 μM PI (Life technologies) in Tyrode's buffer without BSA. The GBS pigment (2.5 μM) or an equivalent amount of control Δ*cylE* extract or 5 μM A23187 was added, and fluorescence intensity was measured for 900 s (15 min) by flow cytometry (LSRII instrument, BD Biosciences). Data were collected using the FACSDiva software system (BD Biosciences) and analyzed by FlowJo (TreeStar).

Treatment of mast cells with inhibitors

PCMCs were pretreated either with pertussis toxin (200 ng/ml; Sigma) for 2 hours or with EGTA (4 mM; Sigma) or LY294002 (100 μM, Sigma) for 30 min in Tyrode's buffer containing 0.1% BSA. Untreated PCMCs were included as controls. Subsequently, the mast cells were centrifuged, washed, and resuspended in Tyrode's buffer without BSA and exposed to either 2.5 μM pigment or an equivalent amount of Δ*cylE* extract or 5 μM A23187 for 1 hour. β-Hex and LDH release was then quantified in mast cell supernatants.

Scanning electron microscopy

About 1×10^6 BMCMCs were centrifuged, washed twice, and resuspended in 0.5 ml of DMEM. BMCMCs were then treated with either 0.5 μM pigment or an equivalent amount of control Δ*cylE* extract or A23187 (0.83 ng/μl, 1.66 μM) for 10 min at 37°C. One volume of Karnovsky's fixative was added to the samples, and the cells were incubated for an additional 10 min at room temperature. Subsequently, the cells were centrifuged and resuspended in 1.4 ml of Karnovsky's fixative and incubated overnight at 4°C. Samples were then prepared for scanning electron microscopy as described (*16*, *65*). Images were captured using a JEOL 5800 scanning electron microscope equipped with a JEOL Orion Digital Acquisition System.

Evaluation of mast cell activation in vivo

Eleven-week-old wild-type C57BL6/J mice ($n = 6$ per group) were intraperitoneally infected with PBS or 10^7 CFU of either wild-type GBS A909 or isogenic Δ*covR* or Δ*covR*Δ*cylE* strains. At 2 hours after infection, peritoneal cells were harvested from the infected mice by injecting 2 ml of PBS containing 10% fetal calf serum into the peritoneal cavity. The abdomen was gently massaged for 30 s, and fluids containing peritoneal cells were aspirated. The peritoneal cells were then cytocentrifuged onto glass slides and stained with May-Grünwald-Giemsa (*24*) to determine activation/degranulation of mast cells. Images were captured in bright field using the Leica DM4000B fluorescence upright microscope. The microscope was attached to a Leica DFC310FX camera, and the acquisition software used was the Leica application suite, version 4.0.0. A representative image from experiments with six mice with similar results is shown (Fig. 4). Blood was also isolated from the infected mice by cardiac puncture and centrifuged to isolate plasma. Histamine release was measured in plasma (10 μl) using the histamine enzyme-linked immunosorbent assay kit (ALPCO) as per the manufacturer's instructions. The experiment was repeated using hyperpigmented Δ*covS*, wild-type GBS NCTC10/84, and isogenic nonpigmented controls Δ*covS*Δ*cyl* and NCTC10/84Δ*cylE*, respectively.

GBS systemic infection

The murine model of GBS systemic infection (*36*) was used to evaluate the role of mast cells. The mast cell–deficient *Cpa3-Cre;Mcl-1*$^{fl/fl}$ mice that exhibit 92 to 100% deficiency in mast cells (*37*) were used. Littermate mast cell–proficient *Cpa3-Cre;Mcl-1*$^{fl/+}$ mice were included as controls. The role of basophils during GBS systemic infection was also examined using basophil-depleted *Mcpt8*^{DTR} mice (*39*). For basophil depletion, *Mcpt8*^{DTR} and control *Mcpt8*$^{+/+}$ mice were injected intraperitoneally with diphtheria toxin (500 ng) as described (*39*), 48 hours before GBS infection (see below).

For GBS systemic infection, 9- to 12-week-old male mice were intraperitoneally injected with 2×10^6 to 2×10^7 CFU of either GBS A909Δ*covR* or isogenic Δ*covR*Δ*cylE*. Blood, peritoneal fluid, and spleens were collected aseptically at 24 hours after infection from the inoculated mice. Spleens were homogenized in sterile PBS, and bacterial counts in spleens and peritoneal fluids were determined by plating serial 10-fold dilutions on TSA as described previously (*36*, *66*). For inflammatory cytokine analysis, organ homogenates were diluted 1:1 in lysis buffer [150 mM NaCl, 15 mM tris, 1 mM $MgCl_2$, 1 mM $CaCl_2$, 1% Triton X-100, supplemented with cOmplete, Mini, EDTA-free protease inhibitor cocktail (Roche)] and incubated overnight at 4°C. The lysates were then centrifuged at 4000*g* for 20 min at 4°C, and the supernatants were stored at −80°C or used immediately for analysis. About 100 μl of sample was used for Luminex bead assays (eBioscience) or ELISA (Cayman Chemicals), and 10 μl of sample was used for histamine analysis as described earlier.

Neutrophils ($Ly6G^+$ $CD11b^+$) in spleens were analyzed by flow cytometry. Spleens were digested with deoxyribonuclease (DNase)/collagenase–containing medium [10% FBS, collagenase (0.8 mg/ml), DNase (0.15 mg/ml) in PBS] for 45 min at 37°C; red blood cells were lysed with lysis buffer (0.15 M NH_4Cl, 1 mM $NaHCO_3$, pH 7.2) for 10 min; and total cell numbers were counted using a hemocytometer as described (*25*). Cells were blocked with unconjugated anti-CD16/CD32 on ice for 10 min and then were stained with allophycocyanin-labeled anti-CD11b (2 μg/ml; BD Biosciences) and phycoerythrin-labeled Ly6G antibodies (1 μg/ml; BD Biosciences) on ice for 15 min. Cells were fixed overnight with 1% paraformaldehyde, and the data were acquired using an LSR II instrument (BD Biosciences). The expression of cell surface markers was analyzed using FlowJo software version 8.8.7 (TreeStar). Gates for subpopulations of cells were based on unstained cells, as well as cells stained with a single color to determine compensation and nonspecific fluorescence.

GBS vaginal colonization

Twelve- to 16-week-old female nonpregnant mast cell–deficient [*Cpa3-Cre;Mcl-1*$^{fl/fl}$ (*37*)] and mast cell–proficient (*Cpa3-Cre;Mcl-1*$^{fl/+}$)

littermate control mice were used to define the role of mast cells in GBS vaginal colonization. Female mast cell–deficient mice and littermate control pairs were synchronized for estrus by cohabiting in the same cage for >10 days if not from birth. Agents such as 17β-estradiol were not administered because these agents have been described to activate mast cells (*50*). Mice were anesthetized using 3 to 4% isoflurane, and GBS A909Δ*covR* or isogenic Δ*covR*Δ*cylE* (1×10^8 to 5×10^8 in 10 μl of sterile PBS) was inoculated into the lower genital tract with a gel loading tip. Mice were left inverted for an additional 5 min under anesthesia. Subsequently, the mice were returned to their cages and monitored until ambulatory. At 4 days after infection, mice were euthanized, and the lower genital tract and uterine horns were excised and analyzed for CFU and mast cell activation. Tissues were homogenized, and GBS CFU were enumerated by serial dilution and plating on both nonselective and selective media [TSA and TSA containing spectinomycin (50 μg/ml)]. Of note, Δ*covR* and Δ*covR*Δ*cylE* strains of GBS are spectinomycin-resistant because *covR* was replaced with a gene conferring spectinomycin resistance in these strains (*20*, *67*). All plates were incubated for 24 hours at 37°C, and the nonselective TSA plates were then left on the bench for an additional 24 to 48 hours to distinguish GBS from other commensal bacteria. As further confirmation, ~100 GBS colonies from each experiment were patched on selective medium (that is, TSA containing spectinomycin), and the level of CAMP factor activity was tested on sheep blood agar plates with the inoculum strain included in parallel. CHROMagar Strep B (DRG International Inc.) was also used to distinguish GBS from commensal organisms. Supernatants of tissue homogenates were analyzed for histamine with the ALPCO histamine ELISA assay as described earlier. For histology, the lower genital tract and uterine horns were excised from mast cell–proficient and mast cell–deficient mice at 4 days after infection. Tissues were fixed in 10% phosphate-buffered formalin at 4°C overnight and stored in 70% ethanol. The tissues were subsequently embedded in paraffin, sectioned, and stained with H&E or toluidine blue. All tissues were mounted and stained by the Histology and Imaging Core located at the University of Washington (Seattle, WA) and were scored by a pathologist blinded to group assignment. Images were captured in bright field with a DM4000B fluorescence upright microscope (Leica) under ×20 and ×40 magnifications. The microscope was attached to a DFC310FX camera (Leica), and the acquisition software used was the Leica application suite (version 4.0.0). The experiment was repeated using natively hyperpigmented wild-type GBS NCTC10/84 and isogenic nonpigmented NCTC10/84Δ*cylE*, using wild-type C57BL6/J mice ($n = 8$ per group).

Statistical analysis

Student's *t* test, Mann-Whitney test, or Bonferroni's, Tukey's, or Dunnett's multiple comparison test following ANOVA, Fisher's exact test, or Barnard's test was used to estimate differences as appropriate, and $P < 0.05$ was considered significant. These tests were performed using GraphPad Prism version 6.0 (GraphPad Software, www.graphpad.com) or SciStatCalc.

SUPPLEMENTARY MATERIALS

Supplementary material for this article is available at http://advances.sciencemag.org/cgi/content/full/1/6/e1400225/DC1

Fig. S1. Hemolytic and CAMP factor activity of two rectovaginal GBS isolates.
Fig. S2. FACS (fluorescence-activated cell sorting) characterization of PCMCs.
Fig. S3. Mast cells release β-hex in a hemolytic pigment dependent manner.
Fig. S4. The GBS pigment and hyperpigmented GBS induce the release of β-hex from BMCMCs derived from NLRP3 knockout mice.
Fig. S5. Mast cells release PGD_2 and LTC_4 in a hemolytic pigment–dependent manner.
Fig. S6. Hyperhemolytic/hyperpigmented GBS and purified pigment activate mast cells to release proinflammatory mediators.
Fig. S7. Time course determination of pigment-mediated β-hex release from mast cells.
Fig. S8. The GBS pigment and hyperpigmented GBS induce the release of the cytosolic enzyme LDH from PCMCs, similar to the Ca^{2+} ionophore.
Fig. S9. Hyperpigmented GBS wild-type NCTC10/84 induces mast cell degranulation in vivo in a hemolytic pigment–dependent manner.
Fig. S10. In vivo mast cell degranulation by hyperpigmented GBSΔ*covS*.
Fig. S11. Bacterial burden and levels of cytokines, neutrophils, and histamine in peritoneal fluids obtained from mast cell–deficient and mast cell–proficient mice during systemic GBS infection.
Fig. S12. Cytokine IL-4 levels were not significantly increased in spleens of mast cell–proficient or mast cell–deficient mice infected with hyperpigmented GBS.
Fig. S13. Basophil-depleted mice exhibit similar bacterial burden and levels of histamine and cytokines during systemic infection with hyperpigmented GBS.
Fig. S14. Decreased vaginal colonization of GBS NCTC10/84 in wild-type mice.

REFERENCES AND NOTES

1. R. Berner, Significance, management and prevention of *Streptococcus agalactiae* infection during the perinatal period. *Expert Rev. Anti Infect. Ther.* **2**, 427–437 (2004).
2. J. E. Lawn, M. G. Gravett, T. M. Nunes, C. E. Rubens, C. Stanton; GAPPS Review Group, Global report on preterm birth and stillbirth (1 of 7): Definitions, description of the burden and opportunities to improve data. *BMC Pregnancy Childbirth* **10** (Suppl. 1), S1 (2010).
3. M. G. Gravett, C. E. Rubens, T. M. Nunes; GAPPS Review Group, Global report on preterm birth and stillbirth (2 of 7): Discovery science. *BMC Pregnancy Childbirth* **10** (Suppl. 1), S2 (2010).
4. J. R. Verani, L. McGee, S. J. Schrag, Prevention of perinatal group B streptococcal disease—Revised guidelines from CDC, 2010. *MMWR Recomm. Rep.* **59**, 1–36 (2010).
5. K. M. Puopolo, Epidemiology of neonatal early-onset sepsis. *NeoReviews* **9**, e571–e579 (2008).
6. F. M. Menzies, M. C. Shepherd, R. J. Nibbs, S. M. Nelson, The role of mast cells and their mediators in reproduction, pregnancy and labour. *Hum. Reprod. Update* **17**, 383–396 (2011).
7. M. Jeziorska, L. A. Salamonsen, D. E. Woolley, Mast cell and eosinophil distribution and activation in human endometrium throughout the menstrual cycle. *Biol. Reprod.* **53**, 312–320 (1995).
8. S. J. Galli, N. Borregaard, T. A. Wynn, Phenotypic and functional plasticity of cells of innate immunity: Macrophages, mast cells and neutrophils. *Nat. Immunol.* **12**, 1035–1044 (2011).
9. A. L. St John, S. N. Abraham, Innate immunity and its regulation by mast cells. *J. Immunol.* **190**, 4458–4463 (2013).
10. M. Urb, D. C. Sheppard, The role of mast cells in the defence against pathogens. *PLOS Pathog.* **8**, e1002619 (2012).
11. D. Carlos, C. Fremond, A. Samarina, V. Vasseur, I. Maillet, S. G. Ramos, F. Erard, V. Quesniaux, H. Ohtsu, C. L. Silva, L. H. Faccioli, B. Ryffel, Histamine plays an essential regulatory role in lung inflammation and protective immunity in the acute phase of Mycobacterium tuberculosis infection. *Infect. Immun.* **77**, 5359–5368 (2009).
12. W. Y. Sun, L. D. Abeynaike, S. Escarbe, C. D. Smith, S. M. Pitson, M. J. Hickey, C. S. Bonder, Rapid histamine-induced neutrophil recruitment is sphingosine kinase-1 dependent. *Am. J. Pathol.* **180**, 1740–1750 (2012).
13. K. Takeshita, K. Sakai, K. B. Bacon, F. Gantner, Critical role of histamine H_4 receptor in leukotriene B_4 production and mast cell-dependent neutrophil recruitment induced by zymosan in vivo. *J. Pharmacol. Exp. Ther.* **307**, 1072–1078 (2003).
14. S. J. Galli, M. Tsai, Mast cells in allergy and infection: Versatile effector and regulatory cells in innate and adaptive immunity. *Eur. J. Immunol.* **40**, 1843–1851 (2010).
15. A. Dahdah, G. Gautier, T. Attout, F. Fiore, E. Lebourdais, R. Msallam, M. Daëron, R. C. Monteiro, M. Benhamou, N. Charles, J. Davoust, U. Blank, B. Malissen, P. Launay, Mast cells aggravate sepsis by inhibiting peritoneal macrophage phagocytosis. *J. Clin. Invest.* **124**, 4577–4589 (2014).
16. C. Whidbey, M. I. Harrell, K. Burnside, L. Ngo, A. K. Becraft, L. M. Iyer, L. Aravind, J. Hitti, K. M. Adams Waldorf, L. Rajagopal, A hemolytic pigment of Group B Streptococcus allows bacterial penetration of human placenta. *J. Exp. Med.* **210**, 1265–1281 (2013).
17. C. Whidbey, J. Vornhagen, C. Gendrin, E. Boldenow, J. M. Samson, K. Doering, L. Ngo, E. A. Ezekwe Jr., J. H. Gundlach, M. A. Elovitz, D. Liggitt, J. A. Duncan, K. M. Adams Waldorf, L. Rajagopal, A

streptococcal lipid toxin induces membrane permeabilization and pyroptosis leading to fetal injury. *EMBO Mol. Med.* **7**, 488–505 (2015).
18. M. C. Lamy, M. Zouine, J. Fert, M. Vergassola, E. Couve, E. Pellegrini, P. Glaser, F. Kunst, T. Msadek, P. Trieu-Cuot, C. Poyart, CovS/CovR of group B streptococcus: A two-component global regulatory system involved in virulence. *Mol. Microbiol.* **54**, 1250–1268 (2004).
19. S. M. Jiang, M. J. Cieslewicz, D. L. Kasper, M. R. Wessels, Regulation of virulence by a two-component system in Group B *Streptococcus*. *J. Bacteriol.* **187**, 1105–1113 (2005).
20. L. Rajagopal, A. Vo, A. Silvestroni, C. E. Rubens, Regulation of cytotoxin expression by converging eukaryotic-type and two-component signalling mechanisms in *Streptococcus agalactiae*. *Mol. Microbiol.* **62**, 941–957 (2006).
21. C. A. Pritzlaff, J. C. Chang, S. P. Kuo, G. S. Tamura, C. E. Rubens, V. Nizet, Genetic basis for the β-haemolytic/cytolytic activity of group B *Streptococcus*. *Mol. Microbiol.* **39**, 236–247 (2001).
22. T. A. Hooven, T. M. Randis, S. C. Daugherty, A. Narechania, P. J. Planet, H. Tettelin, A. J. Ratner, Complete genome sequence of *Streptococcus agalactiae* CNCTC 10/84, a hypervirulent sequence type 26 strain. *Genome Announc.* **2**, e01338-14 (2014).
23. H. W. Wilkinson, R. G. Eagon, Type-specific antigens of group B type Ic streptococci. *Infect. Immun.* **4**, 596–604 (1971).
24. O. Malbec, K. Roget, C. Schiffer, B. Iannascoli, A. R. Dumas, M. Arock, M. Daeron, Peritoneal cell-derived mast cells: An in vitro model of mature serosal-type mouse mast cells. *J. Immunol.* **178**, 6465–6475 (2007).
25. A. M. Piliponsky, C. C. Chen, E. J. Rios, P. M. Treuting, A. Lahiri, M. Abrink, G. Pejler, M. Tsai, S. J. Galli, The chymase mouse mast cell protease 4 degrades TNF, limits inflammation, and promotes survival in a model of sepsis. *Am. J. Pathol.* **181**, 875–886 (2012).
26. M. Akahoshi, C. H. Song, A. M. Piliponsky, M. Metz, A. Guzzetta, M. Abrink, S. M. Schlenner, T. B. Feyerabend, H. R. Rodewald, G. Pejler, M. Tsai, S. J. Galli, Mast cell chymase reduces the toxicity of Gila monster venom, scorpion venom, and vasoactive intestinal polypeptide in mice. *J. Clin. Invest.* **121**, 4180–4191 (2011).
27. A. Costa, R. Gupta, G. Signorino, A. Malara, F. Cardile, C. Biondo, A. Midiri, R. Galbo, P. Trieu-Cuot, S. Papasergi, G. Teti, P. Henneke, G. Mancuso, D. T. Golenbock, C. Beninati, Activation of the NLRP3 inflammasome by group B streptococci. *J. Immunol.* **188**, 1953–1960 (2012).
28. R. Gupta, S. Ghosh, B. Monks, R. Deoliveira, T. Tzeng, P. Kalantari, A. Nandy, B. Bhattacharjee, J. Chan, F. Ferreira, V. Rathinam, S. Sharma, E. Lien, N. Silverman, K. Fitzgerald, A. Firon, P. Trieu-Cuot, P. Henneke, D. Golenbock, RNA and β-hemolysin of Group B *Streptococcus* induce IL-1β by activating NLRP3 inflammasomes in mouse macrophages. *J. Biol. Chem.* **289**, 13701–13705 (2014).
29. V. Supajatura, H. Ushio, A. Nakao, S. Akira, K. Okumura, C. Ra, H. Ogawa, Differential responses of mast cell Toll-like receptors 2 and 4 in allergy and innate immunity. *J. Clin. Invest.* **109**, 1351–1359 (2002).
30. Y. Nakamura, J. Oscherwitz, K. B. Cease, S. M. Chan, R. Muñoz-Planillo, M. Hasegawa, A. E. Villaruz, G. Y. Cheung, M. J. McGavin, J. B. Travers, M. Otto, N. Inohara, G. Nuñez, *Staphylococcus* δ-toxin induces allergic skin disease by activating mast cells. *Nature* **503**, 397–401 (2013).
31. C. M. van Haaster, W. Engels, P. J. Lemmens, G. Hornstra, G. J. van der Vusse, J. W. Heemskerk, Differential release of histamine and prostaglandin D2 in rat peritoneal mast cells: Roles of cytosolic calcium and protein tyrosine kinases. *Biochim. Biophys. Acta* **1265**, 79–88 (1995).
32. J. R. White, T. Ishizaka, K. Ishizaka, R. Sha'afi, Direct demonstration of increased intracellular concentration of free calcium as measured by quin-2 in stimulated rat peritoneal mast cell. *Proc. Natl. Acad. Sci. U.S.A.* **81**, 3978–3982 (1984).
33. G. G. Pendl, E. E. Prieschl, W. Thumb, N. E. Harrer, M. Auer, T. Baumruker, Effects of phosphatidylinositol-3-kinase inhibitors on degranulation and gene induction in allergically triggered mouse mast cells. *Int. Arch. Allergy Immunol.* **112**, 392–399 (1997).
34. M. Aridor, G. Rajmilevich, M. A. Beaven, R. Sagi-Eisenberg, Activation of exocytosis by the heterotrimeric G protein G_{i3}. *Science* **262**, 1569–1572 (1993).
35. S. Nakao, K. Komagoe, T. Inoue, T. Katsu, Comparative study of the membrane-permeabilizing activities of mastoparans and related histamine-releasing agents in bacteria, erythrocytes, and mast cells. *Biochim. Biophys. Acta* **1808**, 490–497 (2011).
36. A. Lembo, M. A. Gurney, K. Burnside, A. Banerjee, M. de los Reyes, J. E. Connelly, W. J. Lin, K. A. Jewell, A. Vo, C. W. Renken, K. S. Doran, L. Rajagopal, Regulation of CovR expression in Group B Streptococcus impacts blood–brain barrier penetration. *Mol. Microbiol.* **77**, 431–443 (2010).
37. J. N. Lilla, C. C. Chen, K. Mukai, M. J. BenBarak, C. B. Franco, J. Kalesnikoff, M. Yu, M. Tsai, A. M. Piliponsky, S. J. Galli, Reduced mast cell and basophil numbers and function in *Cpa3-Cre; Mcl-1*$^{fl/fl}$ mice. *Blood* **118**, 6930–6938 (2011).
38. A. L. Jones, K. M. Knoll, C. E. Rubens, Identification of *Streptococcus agalactiae* virulence genes in the neonatal rat sepsis model using signature-tagged mutagenesis. *Mol. Microbiol.* **37**, 1444–1455 (2000).
39. T. Wada, K. Ishiwata, H. Koseki, T. Ishikura, T. Ugajin, N. Ohnuma, K. Obata, R. Ishikawa, S. Yoshikawa, K. Mukai, Y. Kawano, Y. Minegishi, H. Yokozeki, N. Watanabe, H. Karasuyama, Selective ablation of basophils in mice reveals their nonredundant role in acquired immunity against ticks. *J. Clin. Invest.* **120**, 2867–2875 (2010).
40. S. K. Majeed, Mast cell distribution in mice. *Arzneimittelforschung* **44**, 1170–1173 (1994).
41. K. A. Patras, N. Y. Wang, E. M. Fletcher, C. K. Cavaco, A. Jimenez, M. Garg, J. Fierer, T. R. Sheen, L. Rajagopal, K. S. Doran, Group B Streptococcus CovR regulation modulates host immune signalling pathways to promote vaginal colonization. *Cell. Microbiol.* **15**, 1154–1167 (2013).
42. R. L. Goldenberg, J. C. Hauth, W. W. Andrews, Intrauterine infection and preterm delivery. *N. Engl. J. Med.* **342**, 1500–1507 (2000).
43. T. K. Kobayashi, T. Fujimoto, H. Okamoto, M. Yuasa, I. Sawaragi, Association of mast cells with vaginal trichomoniasis in endocervical smears. *Acta Cytol.* **27**, 133–137 (1983).
44. F. M. Menzies, C. A. Higgins, M. C. Shepherd, R. J. Nibbs, S. M. Nelson, Mast cells reside in myometrium and cervix, but are dispensable in mice for successful pregnancy and labor. *Immunol. Cell Biol.* **90**, 321–329 (2012).
45. Y. Hirai, T. Yasuhara, H. Yoshida, T. Nakajima, M. Fujino, C. Kitada, A new mast cell degranulating peptide "mastoparan" in the venom of *Vespula lewisii*. *Chem. Pharm. Bull.* **27**, 1942–1944 (1979).
46. K. Mizuno, N. Nakahata, Y. Ohizumi, Characterization of mastoparan-induced histamine release from RBL-2H3 cells. *Toxicon* **36**, 447–456 (1998).
47. T. Katsu, M. Kuroko, T. Morikawa, K. Sanchika, H. Yamanaka, S. Shinoda, Y. Fujita, Interaction of wasp venom mastoparan with biomembranes. *Biochim. Biophys. Acta* **1027**, 185–190 (1990).
48. D. Voehringer, Protective and pathological roles of mast cells and basophils. *Nat. Rev. Immunol.* **13**, 362–375 (2013).
49. T. M. Randis, S. E. Gelber, T. A. Hooven, R. G. Abellar, L. H. Akabas, E. L. Lewis, L. B. Walker, L. M. Byland, V. Nizet, A. J. Ratner, Group B *Streptococcus* β-hemolysin/cytolysin breaches maternal-fetal barriers to cause preterm birth and intrauterine fetal demise in vivo. *J. Infect. Dis.* **210**, 265–273 (2014).
50. M. Zaitsu, S. Narita, K. C. Lambert, J. J. Grady, D. M. Estes, E. M. Curran, E. G. Brooks, C. S. Watson, R. M. Goldblum, T. Midoro-Horiuti, Estradiol activates mast cells via a non-genomic estrogen receptor-α and calcium influx. *Mol. Immunol.* **44**, 1977–1985 (2007).
51. M. I. Petrova, E. Lievens, S. Malik, N. Imholz, S. Lebeer, Lactobacillus species as biomarkers and agents that can promote various aspects of vaginal health. *Front. Physiol.* **6**, 81 (2015).
52. M. Parma, V. Stella Vanni, M. Bertini, M. Candiani, Probiotics in the prevention of recurrences of bacterial vaginosis. *Altern. Ther. Health Med.* **20** (Suppl. 1), 52–57 (2014).
53. H. Borgdorff, E. Tsivtsivadze, R. Verhelst, M. Marzorati, S. Jurriaans, G. F. Ndayisaba, F. H. Schuren, J. H. van de Wijgert, Lactobacillus-dominated cervicovaginal microbiota associated with reduced HIV/STI prevalence and genital HIV viral load in African women. *ISME J.* **8**, 1781–1793 (2014).
54. J. Li, J. McCormick, A. Bocking, G. Reid, Importance of vaginal microbes in reproductive health. *Reprod. Sci.* **19**, 235–242 (2012).
55. I. Santi, R. Grifantini, S. M. Jiang, C. Brettoni, G. Grandi, M. R. Wessels, M. Soriani, CsrRS regulates group B *Streptococcus* virulence gene expression in response to environmental pH: A new perspective on vaccine development. *J. Bacteriol.* **191**, 5387–5397 (2009).
56. A. Di Nardo, K. Yamasaki, R. A. Dorschner, Y. Lai, R. L. Gallo, Mast cell cathelicidin antimicrobial peptide prevents invasive group A *Streptococcus* infection of the skin. *J. Immunol.* **180**, 7565–7573 (2008).
57. S. Wernersson, G. Pejler, Mast cell secretory granules: Armed for battle. *Nat. Rev. Immunol.* **14**, 478–494 (2014).
58. F. E. van den Boogaard, X. Brands, J. J. Roelofs, R. de Beer, O. J. De Boer, C. van't Veer, T. van der Poll, Mast cells impair host defense during murine *Streptococcus pneumoniae* pneumonia. *J. Infect. Dis.* **210**, 1376–1384 (2014).
59. H. Sueki, D. Whitaker-Menezes, A. M. Kligman, Structural diversity of mast cell granules in black and white skin. *Br. J. Dermatol.* **144**, 85–93 (2001).
60. Centers for Disease Control and Prevention (CDC), Preterm singleton births—United States, 1989-1996. *MMWR. Morb. Mortal. Wkly. Rep.* **48**, 185–189 (1999).
61. C. Blackmore-Prince, B. Kieke Jr., K. A. Kugaraj, C. Ferré, L. D. Elam-Evans, C. J. Krulewitch, J. A. Gaudino, M. Overpeck, Racial differences in the patterns of singleton preterm delivery in the 1988 National Maternal and Infant Health Survey. *Matern. Child Health J.* **3**, 189–197 (1999).
62. R. C. Lancefield, M. McCarty, W. N. Everly, Multiple mouse-protective antibodies directed against group B streptococci. Special reference to antibodies effective against protein antigens. *J. Exp. Med.* **142**, 165–179 (1975).
63. T. R. Martin, C. E. Rubens, C. B. Wilson, Lung antibacterial defense mechanisms in infant and adult rats: Implications for the pathogenesis of group B streptococcal infections in the neonatal lung. *J. Infect. Dis.* **157**, 91–100 (1988).
64. V. Nizet, R. L. Gibson, E. Y. Chi, P. E. Framson, M. Hulse, C. E. Rubens, Group B streptococcal β-hemolysin expression is associated with injury of lung epithelial cells. *Infect. Immun.* **64**, 3818–3826 (1996).
65. F. Braet, R. De Zanger, E. Wisse, Drying cells for SEM, AFM and TEM by hexamethyldisilazane: A study on hepatic endothelial cells. *J. Microsc.* **186**, 84–87 (1997).
66. K. Burnside, A. Lembo, M. I. Harrell, M. Gurney, L. Xue, N. T. BinhTran, J. E. Connelly, K. A. Jewell, B. Z. Schmidt, M. de los Reyes, W. A. Tao, K. S. Doran, L. Rajagopal, Serine/threonine phosphatase Stp1 mediates post-transcriptional regulation of hemolysin, autolysis, and virulence of group B *Streptococcus*. *J. Biol. Chem.* **286**, 44197–44210 (2011).
67. W. J. Lin, D. Walthers, J. E. Connelly, K. Burnside, K. A. Jewell, L. J. Kenney, L. Rajagopal, Threonine phosphorylation prevents promoter DNA binding of the Group B Streptococcus response regulator CovR. *Mol. Microbiol.* **71**, 1477–1495 (2009).

Acknowledgments: We are grateful to the women who participated in this study. We thank H. Karasuyama at Tokyo Medical and Dental University for the *Mcpt8*^{DTR} mice; D. Liggitt for his expert advice; M. Chan for assistance with animal experiments; and P. Truong, L. Campos, P. Quach, and V. Allishetti for technical assistance. **Funding:** This work was supported by funding from NIH grants R01AI112619 and R21AI109222 (to L.R.), R01AI100989 (to L.R. and K. A. W.), and R01HL113351 (to A. M. P.). C.W. and J.V. were supported by NIH training grant (T32 AI007509, Principal Investigator: Lee Ann Campbell). The content is solely the responsibility of the authors and does not necessarily represent the official views of NIH. Scanning electron microscopy was performed at the Fred Hutch Cancer Research Center. **Author contributions:** C.G., J.V., L.N., C.W., E.B., V.S.-U., M.C., K.B., and A.M.P. performed the experiments; D.P.G. collected and provided GBS strains; C.G., J.V., L.N., C.W., A.M.P., and L.R. designed the research; C.G., J.V., L.N., C.W., K.B., D.P.G., K.A.W., A.M.P., and L.R. analyzed the results and wrote the paper. **Competing interests:** The authors declare that they have no competing interests.

Submitted 16 December 2014
Accepted 4 June 2015
Published 17 July 2015
10.1126/sciadv.1400225

Citation: C. Gendrin, J. Vornhagen, L. Ngo, C. Whidbey, E. Boldenow, V. Santana-Ufret, M. Clauson, K. Burnside, D. P. Galloway, K. A. Waldorf, A. M. Piliponsky, L. Rajagopal, Mast cell degranulation by a hemolytic lipid toxin decreases GBS colonization and infection. *Sci. Adv.* **1**, e1400225 (2015).